WIND-TUNNEL RESEARCH ON THE MECHANICS OF PLUMES IN THE ATMOSPHERIC SURFACE LAYER

PART III

by

M. Poreh[1] and J. E. Cermak[2]

FLUID MECHANICS AND
WIND ENGINEERING PROGRAM

COLLEGE OF ENGINEERING

COLORADO STATE UNIVERSITY
FORT COLLINS, COLORADO

WIND-TUNNEL RESEARCH ON THE MECHANICS OF PLUMES IN THE ATMOSPHERIC SURFACE LAYER

PART III

by

M. Poreh[1] and J. E. Cermak[2]

WIND-TUNNEL STUDY OF DIFFUSION AND DEPOSITION OF PARTICLES WITH APPRECIABLE SETTLING VELOCITIES

-ANNUAL REPORT-

prepared for

Department of the Army
U.S. Army Armament Research and Development Command
Chemical Systems Laboratory
Aberdeen Proving Ground, Maryland 21010

Fluid Mechanics and Wind Engineering Program
Fluid Dynamic and Diffusion Laboratory
Colorado State University
Fort Collins, Colorado 80523

May 1985

CER84-85MP-JEC48
Project No. 5-32512

[1]Visiting Professor, Wind Engineering Scholar for 1984-85, Colorado State University.
[2]Professor, Fluid Mechanics and Wind Engineering Program

Unclassified
SECURITY CLASSIFICATION OF THIS PAGE

REPORT DOCUMENTATION PAGE

1a. REPORT SECURITY CLASSIFICATION Unclassified	1b. RESTRICTIVE MARKINGS
2a. SECURITY CLASSIFICATION AUTHORITY	3. DISTRIBUTION / AVAILABILITY OF REPORT
2b. DECLASSIFICATION / DOWNGRADING SCHEDULE NA	
4. PERFORMING ORGANIZATION REPORT NUMBER(S)	5. MONITORING ORGANIZATION REPORT NUMBER(S)
6a. NAME OF PERFORMING ORGANIZATION Fluid Dynamics & Diffusion Lab. 6b. OFFICE SYMBOL *(If applicable)*	7a. NAME OF MONITORING ORGANIZATION CDR/DIR
6c. ADDRESS *(City, State, and ZIP Code)* Department of Civil Engineering Colorado State University Fort Collins, Colorado 80523	7b. ADDRESS *(City, State, and ZIP Code)* Chemical Systems Laboratory Attn: DRDAR-CLB-PS (Dr. E. Stuebing) Aberdeen Proving Ground, Maryland 21010
8a. NAME OF FUNDING / SPONSORING ORGANIZATION 8b. OFFICE SYMBOL *(If applicable)*	9. PROCUREMENT INSTRUMENT IDENTIFICATION NUMBER
8c. ADDRESS *(City, State, and ZIP Code)*	10. SOURCE OF FUNDING NUMBERS PROGRAM ELEMENT NO. / PROJECT NO. / TASK NO. / WORK UNIT ACCESSION NO.

11. TITLE *(Include Security Classification)*
Wind-Tunnel Research on the Mechanics of Plumes in the Atmospheric Surface Layer, Part III: Wind-Tunnel Study of Diffusion and Deposition of Particles with Appreciable Settling Velocities

12. PERSONAL AUTHOR(S)
M. Poreh and J. E. Cermak

13a. TYPE OF REPORT	13b. TIME COVERED	14. DATE OF REPORT *(Year, Month, Day)*	15. PAGE COUNT
Final Report	FROM ______ TO ______	1985 May	40

16. SUPPLEMENTARY NOTATION
The findings in this report are not to be construed as an official Department of the Army position, unless so designated by other authorized documents.

17. COSATI CODES			18. SUBJECT TERMS *(Continue on reverse if necessary and identify by block number)*
FIELD	GROUP	SUB-GROUP	

19. ABSTRACT *(Continue on reverse if necessary and identify by block number)*

The deposition on a smooth surface of particles with appreciable settling velocities V_g and small Froude numbers Vg^2/gh, where h is the height of the source in a neutrally stable boundary layer, was studied in a meteorological wind tunnel. The measured longitudinal deposition rates of the deposited particles were closely predicted by an approximate model, which relates the deposition rate of settling particle plumes to the diffusion of passive plumes with no reflection from the ground. The lateral dispersion rates of the settling particle plumes were found, however, to be smaller than those of passive plumes.

20. DISTRIBUTION / AVAILABILITY OF ABSTRACT ☐ UNCLASSIFIED/UNLIMITED ☐ SAME AS RPT. ☐ DTIC USERS	21. ABSTRACT SECURITY CLASSIFICATION
22a. NAME OF RESPONSIBLE INDIVIDUAL	22b. TELEPHONE *(Include Area Code)* / 22c. OFFICE SYMBOL

DD FORM 1473, 84 MAR — 83 APR edition may be used until exhausted. All other editions are obsolete.

SECURITY CLASSIFICATION OF THIS PAGE

ABSTRACT

The deposition on a smooth surface of particles with appreciable settling velocities V_g and small Froude numbers V_g^2/gh, where h is the height of the source in a neutrally stable boundary layer, was studied in a meteorological wind tunnel. The measured longitudinal deposition rates of the deposited particles were closely predicted by an approximate model, which relates the deposition rate of settling particle plumes to the diffusion of passive plumes with no reflection from the ground. The lateral dispersion rates of the settling particle plumes were found, however, to be smaller than those of passive plumes.

KEY WORDS

Deposition, Particles, Dispersion, Atmospheric Diffusion, Particle Plumes, Gaussian Models, Wind-Tunnel Simulation

CONTENTS

Page

1. INTRODUCTION 2

2. WIND-TUNNEL SIMULATION OF PARTICLE-PLUMES IN A NEUTRALLY STABLE ATMOSPHERIC SURFACE LAYER 3

2.1 General 3
2.2 The Case of Small Froude Numbers 4
2.3 Characteristic Response Times of Particles 4
2.4 The Range of Froude Number Independence 7

3. A MODEL FOR THE DEPOSITION OF PARTICLE PLUMES 9

3.1 General 9
3.2 On the Values of σ_z and σ_y 11

4. EXPERIMENTAL FACILITIES, PROCEDURES AND THE EXPERIMENTAL PROGRAM 13

4.1 Wind Tunnel 13
4.2 Particles 13
4.3 The Velocity Profile in the Wind Tunnel 16
4.4 Deposition Measurements 16
4.5 The Experimental Program 20

5. ANALYSIS OF THE RESULTS 25

5.1 The Analytical Model 25
5.2 The Measured Longitudinal Deposition 29
5.3 The Measured Lateral Diffusion 38
5.4 Conclusions and Recommendations 39

LITERATURE CITED 40

LIST OF TABLES

Page

1. The Experimental Program 20

2. The Experimental Results 21

LIST OF FIGURES

Page

1. Meteorological Wind Tunnel, Fluid Dynamics and Diffusion Laboratory, Colorado State University 14

2. Experimental configurations for (a) sorting the particles and (b) determining their average fall-velocity 15

3. Mean velocity and turbulence profiles in the wind tunnel 17

4. Typical lateral distribution of particles 18

5. Measured values of $\sigma_y(x^*)$ in three identical runs 19

6. The dependence of the position of maximum deposition x^*_{max} on V_g/U 26

7. The dependence of $P(x^*)_{max}$ on V_g/U 27

8. The dimensionless distribution $P(x^*)$ for different velocity ratios and different source heights 28

9. The effect of V/U_g on the longitudinal deposition of particles (Eq. (53)) 30

10. The effect of small changes in V_g/U on $P(x^*)$ 31

11. The combined distributions of two equal mono-dispersed groups of particles with fall velocities $V_g/U = 0.1(1 \pm \varepsilon)$ 32

12-13. The longitudinal deposition of the particles ($V_g/U = 0.1$, $h/\delta = 0.5$) 33

14-17. The longitudinal deposition of particles $P(x^*)$ 34

18-21. The longitudinal deposition of particles $P(x^*)$ 35

22. The lateral dispersion of particles (Runs 1-17) 36

WIND-TUNNEL RESEARCH ON THE MECHANICS OF PLUMES IN THE ATMOSPHERIC SURFACE LAYER

1 INTRODUCTION

Atmospheric diffusion and deposition on the ground of particle-plumes with appreciable settling (free-fall) velocities emitted from elevated sources is of considerable importance in many problems.

The motion and the diffusion of such particles in a turbulent field are very complex phenomena. They are affected by the size of the particles, relative to the size of the turbulent eddies, their inertia and added mass, the turbulent velocity field and the crossing of the turbulent eddies by the free-falling particles, which attenuates their diffusion relative to that of ideal tracers. Similarly, the deposition rate of particles on the ground is a function of their concentration near the ground, the settling velocity, the detailed nature of turbulence near the ground, the surface roughness and the forces between the surface and the particulates at very small distances. Due to the complexity of the problem, it is usually treated by approximate semi-empirical models, which have many restrictions. Evaluation of such models, as well as the ability to develop improved models, depend on the availability of experimental data. Due to the inherent difficulties and high cost of full-scale atmospheric diffusion experiments, such data is, however, very difficult to obtain.

Similar difficulties of studying atmospheric flows and atmospheric diffusion of gases have stimulated the use of specially designed wind tunnels for physical simulation of these phenomena.

This work is a preliminary attempt to study some cases of diffusion of particulates in a neutral atmosphere by physical simulation in a meteorological wind tunnel. Preliminary analysis has revealed certain limitations and constraints of such physical simulation (Poreh and Cermak, 1984).[11] The experimental work of the current study was therefore restricted to the simpler case of small particles with appreciable settling velocities, diffusing from elevated sources in a neutral turbulent boundary layer over a smooth, sticky surface. These restrictions eliminate reflection of particles from the surface and re-entrainment into the air stream.

The report discusses the necessary criteria for the simulation of particle-plumes in wind tunnels, describes the experimental techniques and procedures used in the study, presents the results of the simulation as well as a very simple statistical model which exhibits the effect of the basic parameters on the ground-level distribution of particulates.

2 WIND-TUNNEL SIMULATION OF PARTICLE-PLUMES IN A NEUTRALLY STABLE ATMOSPHERIC SURFACE LAYER

2.1 General

Simulation of diffusion in wind-tunnel models requires, of course, that the surface-layer flow be correctly simulated in the model. The requirements for simulating neutrally-stable flows are well known (Cermak, 1971, 1975).[2,3] In summary, they are: matching the mean and turbulent flow characteristics of the Atmospheric Surface Layer (ASL) with those of the wind-tunnel boundary layer, up to a height of the order of 4 times the height of the investigated layer, or, when the entire ASL is simulated, up to the edge of the surface boundary layer, which on the average is estimated to be of the order of 600 m (Counihan, 1974).[6] This is achieved by using relatively long wind-tunnel test sections, and installing spires or vortex generators at the entrance to the test section, to produce the appropriate momentum deficiency and to roughly match, as early as possible, the velocity distributions in the upstream section of the model and the ASL. The equivalent roughness and topography in the physical model are then matched with the prototype roughness and topography using the same geometric scale, R_L, for δ, for the roughness and for the topography

$$R_L = \frac{\delta_m}{\delta_p} = \frac{Zo_m}{Zo_p} = \frac{L_m}{L_p} \quad . \qquad (1)$$

If the Reynolds number in the model is sufficiently large, so that

$$\frac{V^* Zo_m}{\nu} > 10 \qquad (2)$$

where V^* is the shear velocity, and

$$\frac{U\delta}{\nu} > 10^5 \qquad (3)$$

where U is the mean velocity, the dimensionless mean and turbulent velocity distributions in the model, after a certain distance, of the order of 10 δ, from the beginning of the test section will be approximately similar to those in the lower part of the ASL, provided R_L is sufficiently small ($<$ 0.01).

The above requirements are also sufficient for approximate simulation of the diffusion of passive tracers in a neutral ASL up to a distance of approximately 5 kms (Cermak, 1975).[3]

To simulate the diffusion of particles with appreciable settling velocity V_g, it is also required to match in the model and in the atmosphere the following dimensionless parameters:

(1) The settling velocity ratio, V_g/U,

(2) The Froude number, V_g^2/gL, and

(3) The Reynolds number of the relative motion of these particles.

It is relatively easy to meet the first requirement. The second requirement implies that the velocity scale in the model must be proportional to the square root of the geometric scale. This requirement implies that the value of the Reynolds numbers in the small-scaled model would in many cases be below the critical value required for a correct simulation of the turbulence in the ASL.

There are, however, some important cases for which the requirements (2) and (3) need not be matched in the model and thus approximate simulations of the diffusion and ground deposition of the particulates can be obtained by matching only the dimensionless velocity ratio (1).

2.2 The Case of Small Froude Numbers

The dimensionless Froude number V_g^2/gL may be interpreted to be the ratio of the particle response time (or distance) to the characteristic time (or size) of the turbulent eddies. When the particle response time is very short, compared to the characteristic time of the turbulence, during which significant changes in the velocity field seen by the particle occur, the particle will be in a local equilibrium with the flow and, in the limiting case of $V_g^2/gL \to 0$, the velocity of the particle will be equal to the vectorial sum of the local velocity and the settling velocity;

$$\vec{V} = \vec{U} - V_g\vec{k} \quad . \tag{4}$$

In this case, the dispersion of the particles is expected to be independent of both the Froude number and the particle Reynolds number. Cases of very small Froude numbers are frequently encountered in many environmental phenomena and thus wind-tunnel simulation of such cases is of considerable interest.

2.3 Characteristic Response Times of Particles

The motion of a solid particle in an unsteady velocity field may be approximately described by the following equation (Soo, 1967)[13]:

$$\frac{\pi}{6} d^3 \rho_p \frac{D}{Dt} \vec{V} = \frac{\pi d^2}{4} \frac{\rho}{z} C_D (\vec{U} - \vec{V}_p) \left| U - V_p \right|$$

$$+ \frac{\pi}{6} d^3 (\rho_p - \rho)\vec{g} + \frac{1}{2} \frac{\pi}{6} d^3 \rho \frac{D}{Dt} (\vec{U} - \vec{V}) \tag{5}$$

This equation neglects the effect of the pressure gradient as well as that of the so-called Busset-history-term, which might be important under conditions of high acceleration and when the particles and fluid densities are of the same order of magnitude. When $\rho_p >> \rho$, the last term in Eq. (5), which describes the effect of the added mass on the particle acceleration, may also be neglected, and the equation of motion can be written as:

$$\frac{d}{dt} (\vec{V}) = - g \vec{k} - \frac{3}{4} \frac{\rho}{\rho_p} \frac{C_D}{d} \left| \vec{V} - \vec{U} \right| \cdot (\vec{V} - \vec{U}) \tag{6}$$

The drag coefficient is a function of the Reynolds number of the relative particle motion, $Re = |\bar{V} - \bar{U}| \cdot d/\nu$. This function can usually be described, within a certain range of Reynolds numbers, as a power law:

$$C_D = C \cdot Re^{-n} \tag{7}$$

The power n in this equation is 1 for small Reynolds numbers and 0 for large Reynolds numbers.

We shall define the response time of particles with appreciable settling velocity by considering the motion of particles whose speed is close to their settling velocity. Consider a particle that at $t = 0$ is moving in stagnant air at a speed

$$\vec{V} = - V_g [(1 + \varepsilon_z(o))\vec{k} + \varepsilon_y(o)\vec{j}] \quad . \tag{8}$$

The decay of both $\varepsilon_z(t)$ and $\varepsilon_y(t)$ may be calculated from Eq. (5). Using the power law approximation for C_D one finds from Eq. (5) that

$$\frac{d\vec{V}}{dt} = - g\vec{k} - \frac{3}{4} \frac{\rho \, C\nu^{n} \, V_g^{2-n}}{\rho_p \; d^{1+n}} [(1+\varepsilon_z)^2 + \varepsilon_y{}^2]^{(1-n)/2} \cdot [(1+\varepsilon_z)]\vec{k} + \varepsilon_y\vec{j}] \tag{9}$$

At large t, both ε_z and ε_y are zero so that

$$V_g = \left(\frac{4g}{3C} \frac{\rho_p}{\rho} \frac{d^{1+n}}{\nu n} \right)^{1/(2-n)} \tag{10}$$

and one may rewrite Eq. (9) as

$$-\frac{V_g}{g} \frac{d}{dt} (\varepsilon_z \bar{k} + \varepsilon_y j) = -\bar{k} + [(1+\varepsilon_z)^2 + \varepsilon_y{}^2]^{(1-n)/2} [(1+\varepsilon_z)\vec{k} + \varepsilon_y \vec{j}] \tag{11}$$

Separating the two acceleration components, one finds that for small ε_z and ε_y,

$$\frac{d\varepsilon_y}{dt} = - \frac{g}{V_g} \varepsilon_y \tag{12}$$

and

$$\frac{d\varepsilon_z}{dt} = - \frac{g}{v} (2-n) \varepsilon_z \tag{13}$$

The solutions of these equations are

$$\varepsilon_y(t) = \varepsilon_y(o) \exp[-t/(V_g/g)] \tag{14}$$

and

$$\varepsilon_z(t) = \varepsilon_z(o) \exp[-(2-n)t/(V_g/g)] \tag{15}$$

One may thus define two characteristic response times T_y and T_z, which are measures of the time it takes particles falling at a relative speed V_g, to adjust to new field conditions, as

$$T_y = \frac{V_g}{g} \tag{16}$$

and

$$T_z = \frac{V_g}{(2-n)g} \tag{17}$$

One may also conclude from the above analysis that when the Reynolds number of the relative motion of particle is small (n = 1), the response of the particles will be isotropic, namely,

$$T_y = T_z = T = \frac{V_g}{g} \tag{18}$$

We shall refer to T as the <u>nominal response time</u> of the particles.

When the Reynolds number increases and the inertial effects become significant, n decreases and the response time of the particles to horizontal velocity, which changes according to Eq. (17), would be larger than its response to vertical velocity fluctuations. For very large Reynolds numbers (n = 0) the ratio between the horizontal and vertical response times will be 2.

2.4 The Range of Froude Number Independence

We assume that when the response time of the free falling particles is small compared to the time it takes the particles to cross the energy-containing eddies, the diffusion process would be independent of both the Froude number and the particle's Reynolds number.

Denoting by ℓ, the smallest significant eddy size and assuming that a characteristic travel time of a particle within this eddy is ℓ/V_g, our assumption should be valid when

$$\frac{V_g^2}{g\ell} = k << 1 \ . \qquad (19)$$

Csanady (1963),[7] (also see Pasquill, (1974),[10] p. 152), estimated that the particle would fully respond to the turbulent motion when

$$\frac{V_g^2}{g\ell} < \frac{1}{2\pi} \ . \qquad (20)$$

The diffusion of a continuous plume from an elevated source at a height h above the ground is primarily determined by the energy containing eddies whose size is of the order of h. If one neglects the contribution to the diffusion process of eddies whose size is

$$\ell < 0.2\ h \ , \qquad (21)$$

one finds that the effect of $V_g^2/g\ell$ may be neglected when

$$\frac{V_g^2}{gh} < 0.0328 \ . \qquad (22)$$

Another criterion related to the effect of the fall velocity on diffusion has been derived by Smith (1961),[12] (also see Pasquill, (1974), pp. 135-151).[10] According to Smith, the long-time growth of a cluster of particles descending in a turbulent field is attenuated by the factor $(1 + \beta^2V_g^2/(U^2)^{1/4}$, where β is the ratio of the Lagrangian to the Eulerian integral time scales. For $\beta = 5$ and

$$\frac{V_g}{U} < 0.1 , \qquad (23)$$

the effect of the fall velocity on the expansion rate of a cluster is expected to be smaller than 10 percent. The effect of the fall velocity on continuous particle plumes is expected to be smaller than its effect on clusters. Thus, it will be assumed at this stage, that when both Eq. (22) and Eq. (23) are satisfied, the diffusion of a continuous particle plume can be independent of the Froude number and of the particle's Reynolds number. It also follows that approximate simulations of the diffusion of such plumes can be obtained by matching only the ratio of the velocity ratio V_g/U in the model and atmosphere.

Such approximate simulations will not include, of course, the full effect of turbulent eddies which are much smaller than 0.2 h. For this reason, they cannot be used to study the relative diffusion of clouds (two-particle diffusion problems), where the effect of the small eddies cannot be neglected.

3 A MODEL FOR THE DEPOSITION OF PARTICLE PLUMES

3.1 General

Models for diffusion and deposition of particle plumes, composed of particles with appreciable settling velocities, are generally based on similar models for diffusion of passive tracers. They either use the differential equation describing the mean conservation of mass together with some type of closure, such as the K-Theory (Godson, 1958),[8] or they use a statistical approach like the Gaussian model (Csanady, 1963;[7] Overcamp, 1976).[9]

Gaussian models are widely used for predicting dispersion of passive tracers and we have therefore decided to analyze our experimental data using the simplest possible Gaussian model. The simplest available Gaussian models are based on the assumption that the vertical distributions of particle plumes can be described by a Gaussian function, except that the plumes tilt down at a slope of V_g/U, where V_g is the settling velocity. The use of such models has turned out, however, to be problematic, due to the boundary conditions at ground level. Chamberlain (1953)[5] proposed that the rate of deposition on the ground is proportional to the ground-level concentration (the concentration in the air just above the ground). The constant of proportionality is the deposition velocity V_d which has to be determined from experiments or theory. In addition, one has to account for the effect of the ground on the plume, which is described in the case of passive tracers ($V_g = 0$) emitted from $z = h$ by an image source at $z = -h$. In cases when $V_d \neq V_g$ the adoption of these assumptions violate the mass conservation equation and complicated models were developed to calculate the appropriate strength of an image area source which will satisfy the conservation of mass (Overcamp, 1976).[9]

Since the present study is limited to the case of particles with appreciable fall velocity, one can simply overcome this problem by considering only the motion of the real plume and completely ignore the image plume and the assumption of Chamberlain. Furthermore, since we limit the study to small Froude numbers, the values of σ_z and σ_y are assumed to be the same as in corresponding cases of passive particles.

Consider an ASL in which the diffusion of a tracer from an elevation is described by

$$C^y(x,z) = \frac{Q}{(2\pi)^{\frac{1}{2}}\sigma_z U} \exp\left(-\frac{(h-z)^2}{2\sigma_z^2}\right) \quad (24)$$

where C^y is the cross-wind integrated concentration

$$C^y = \int_{-\infty}^{\infty} C(y)dy \quad . \quad (25)$$

Since the lateral diffusion is usually Gaussian, namely

$$C(y) = C_{max} \exp(- \frac{y^2}{2\sigma_y^2}) \quad , \tag{26}$$

the cross-wind integrated concentration is given by

$$C^y = (2\pi)^{\frac{1}{2}} \cdot C_{max} \sigma_y \quad . \tag{27}$$

The probability of a particle emitted at h to pass, at a given distance x between the elevations z and z+dz is given by

$$P(z)dz = \frac{1}{\sqrt{2\pi}\ \sigma_z(x)} \exp\left(- \frac{(h - z)^2}{2\sigma_z^2}\right) dz \tag{28}$$

Since particles in a particle-plume are on the average settling down at a velocity V_g, we shall assume that the probability of particles depositing between x and x+dx is equal to the probability P(z)dz for $z = V_g x/U$ and $dz = (V_g/U)dx$. Substitution in Eq. (28) gives:

$$P_x = \frac{1\ V_g}{\sqrt{2\pi}\ \ \sigma_z U} \exp\left[- \frac{(h - \frac{V_g}{U} x)^2}{2\sigma_z^2}\right] \tag{29}$$

It must be realized that this model is an approximate one and should be limited to large values of fall velocities, as Eq. (29) does not exactly satisfy the continuity equation. Namely

$$\int_{-\infty}^{\infty} P_x dx = 1 + E \quad , \tag{30}$$

where E is an error which depends on $\sigma_z(x)$ and V_g/U.

Numerical integration of Eq. (30) for the experimental range $0.11 < V_g/U < 0.045$ shows that for this range $E \leqq +3\%$. The error increases for smaller values of V_g/U ($E = 10\%$ at $V_g/U = 0.006$). It also increases when the rate of growth of σ_z with x does (see Eq. (38)).

At any rate, the errors for relatively large full velocities are estimated to be much smaller than the uncertainties in the values of the various variables or the accuracy of the Gaussian model (Eq. (24)). Thus, the mass inconsistency of the model will be ignored at this stage.

Using dimensionless variables

$$\sigma^* = \sigma/h \quad \text{and} \quad x^* = x/h \tag{31}$$

Eq. (29) becomes

$$P(x^*) = \frac{V_g/U}{\sqrt{2\pi}\sigma_z^*} \exp\left[-\frac{(1-\frac{V_g}{U}\frac{x}{h})^2}{2\sigma_2^{*2}}\right] \tag{32}$$

A particle-plume with $\sigma_z \rightarrow 0$ will deposit according to Eq. (29) at

$$\frac{x\,V_g}{h\,U} = 1 \quad . \tag{33}$$

If the velocity in the boundary layer is described by a power law

$$\frac{u}{U_{REF}} = \left(\frac{z}{Z_{REF}}\right)^m \tag{34}$$

where m is a positive number (usually between 0.1 and 0.3). A plume with $\sigma_z \rightarrow 0$ would deposit in such a velocity field at a closer distance

$$\frac{x}{h}\frac{V_g}{U} = \frac{1}{(1+m)}$$

To account for this effect, we shall replace Eq. (33) by

$$P(x^*) = \frac{(1+m)V_g/U}{\sqrt{2\pi}\ \sigma_z^*} \exp\left[-\frac{(1-(1+m)\frac{V_g}{U}\frac{x}{h})^2}{2\sigma_z^{*2}}\right] \tag{35}$$

3.2 On the Values of σ_z and σ_y

The value of σ_z, for both passive tracers and particulates, is expected to be determined by the atmospheric stability, the surface roughness (Z_o) the thickness of the atmospheric boundary layer (δ) and the height of the source (h). Thus, for a given stability and surface roughness, one expects to find in the literature dimensionless expressions for σ such as

$$\frac{\sigma}{\delta} = F\left(\frac{x}{\delta}, \frac{h}{\delta}\right) \quad . \tag{36}$$

Instead, both $\sigma_z(x)$ and $\sigma_y(x)$ are generally described by dimensionally non-homogeneous functions of x and y. Within a limited range of x it is usually assumed that

$$\sigma_z = ax^b \qquad \text{and} \qquad \sigma_y = cx^d \tag{37}$$

where a, b, c, and d are independent of h and δ. We shall also assume that σ_z and σ_y in the atmosphere are approximately independent of h and use, for length scales in meters, the values

$$a = 0.62 \qquad b = 0.6 \qquad c = 0.23 \qquad \text{and} \qquad d = 0.85 \tag{38}$$

which provide a good approximation, in the range of $10^3 < x(m) < 10^4$, to the equations proposed by Briggs (1973)[1] for diffusion in a neutral atmosphere for open country. We shall, however, assume that σ is a function of the boundary layer thickness δ which is of the order of 600 m in the atmosphere (Counihan, 1974),[6] in correlating the atmosphere and the wind tunnel, where δ is of the order of 1 m. Accordingly we assume that

$$\frac{\sigma_z}{\delta} = k\left(\frac{x}{\delta}\right)^b \qquad \text{and} \qquad \frac{\sigma_y}{\delta} = e\left(\frac{x}{\delta}\right)^d \tag{39}$$

where

$$k = a(600)^{b-1} = 0.048$$

and

$$e = C(600)^{d-1} = 0.088.$$

The dimensionless spread σ_z^* is thus given by

$$\sigma_z^* = \frac{\sigma_z}{h} = k\left(\frac{\delta}{h}\right)^{1-b} x^{*b} \quad . \tag{40}$$

4 EXPERIMENTAL FACILITIES, PROCEDURES AND THE EXPERIMENTAL PROGRAM

4.1 Wind Tunnel

The experiments were conducted in the Meteorological Wind Tunnel (MWT) at Colorado State University. Design and operation of the wind tunnel are described in detail by Cermak (1981).[4] Elevation and plan views of the MWT are shown in Figure 1.

A very fine screen was installed at the entrance to the MWT test section. The screen produced a considerable pressure drop, which reduced the pressure in the test section below pressure outside the tunnel.

Spires were installed downstream of the screen during the diffusion tests to produce a third turbulent boundary layer in the tunnel.

4.2 Particles

Expanded polystyrene particles of an average diameter of 1 mm were used in this study. The particles, supplied by the Department of Research and Development, Arco Chemical Company, Newtown Square, Pennsylvania, were initially sorted into groups by the following procedure. The particles were released from an elevated source in a uniform flow and allowed to deposit on the floor of a small wind-tunnel, which was covered with open elongated containers, as shown in Figure 2(a). The fall velocity, of the groups of particles found in each container, was initially estimated by $V_g = Uh/\bar{x}$. About 200 particles from each group were then released from a 4 mm ID brass tube installed in the MWT at an angle $\alpha = \tan(V_g/U)$ (see Figure 2b). The brass tube was connected to a plastic tube which ended outside the tunnel. The difference between the outside pressure and the pressure in the test section produced a flow of air in the tube which was adjusted, by changing the length of the tube, to produce an average exit velocity of the order of U.

The tube acted like a small vacuum cleaner and the particles were easily sucked in by the tube and then injected in the tunnel. The nominal fall velocity of each group of particles was then corrected using the average deposition distance in this experiment. The distribution of the particles suggested that the fall velocities in each group were distributed in the range $V_g(1 \pm E)$, where V_g is the average fall velocity. The value of E was approximately 0.10 for the groups of particles with fall velocities of the order of 0.3 m/s. It was, however, much larger for groups of particles with fall velocities of the order of 0.6 m/s, since the ratio of the width of the containers, shown in Figure 2(a), to the distance $\bar{x}$, was in these cases larger.

The distance $\bar{x}$ in this configuration was on the average 2.5 m and $h/\bar{x}$ varied between 0.12 m to 1.5 m.

It is estimated that the accuracy of this procedure for determining the average value of V_g for each group is of the order of 7 percent.

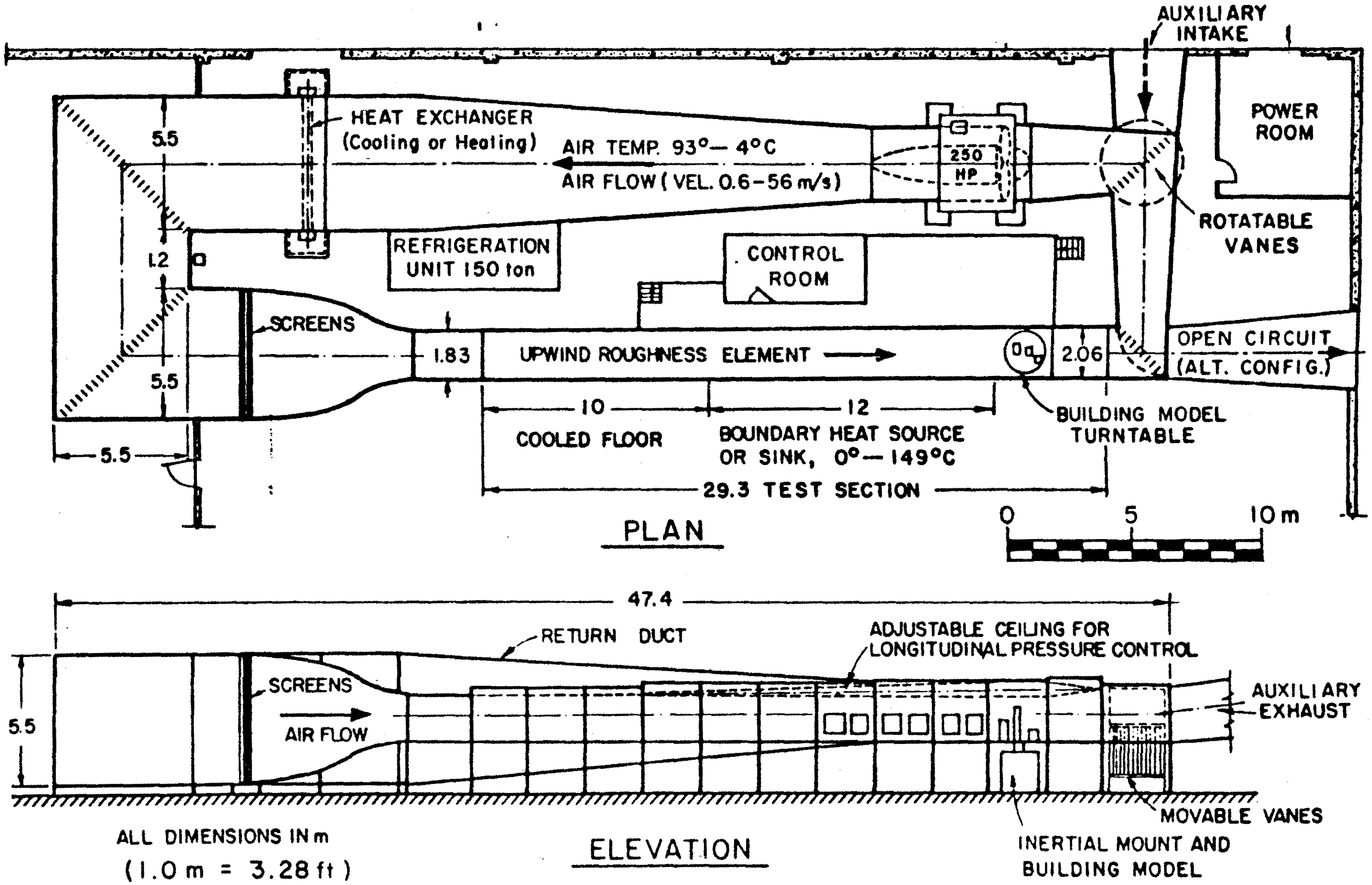

Figure 1. Meteorological Wind Tunnel, Fluid Dynamics and Diffusion Laboratory, Colorado State University

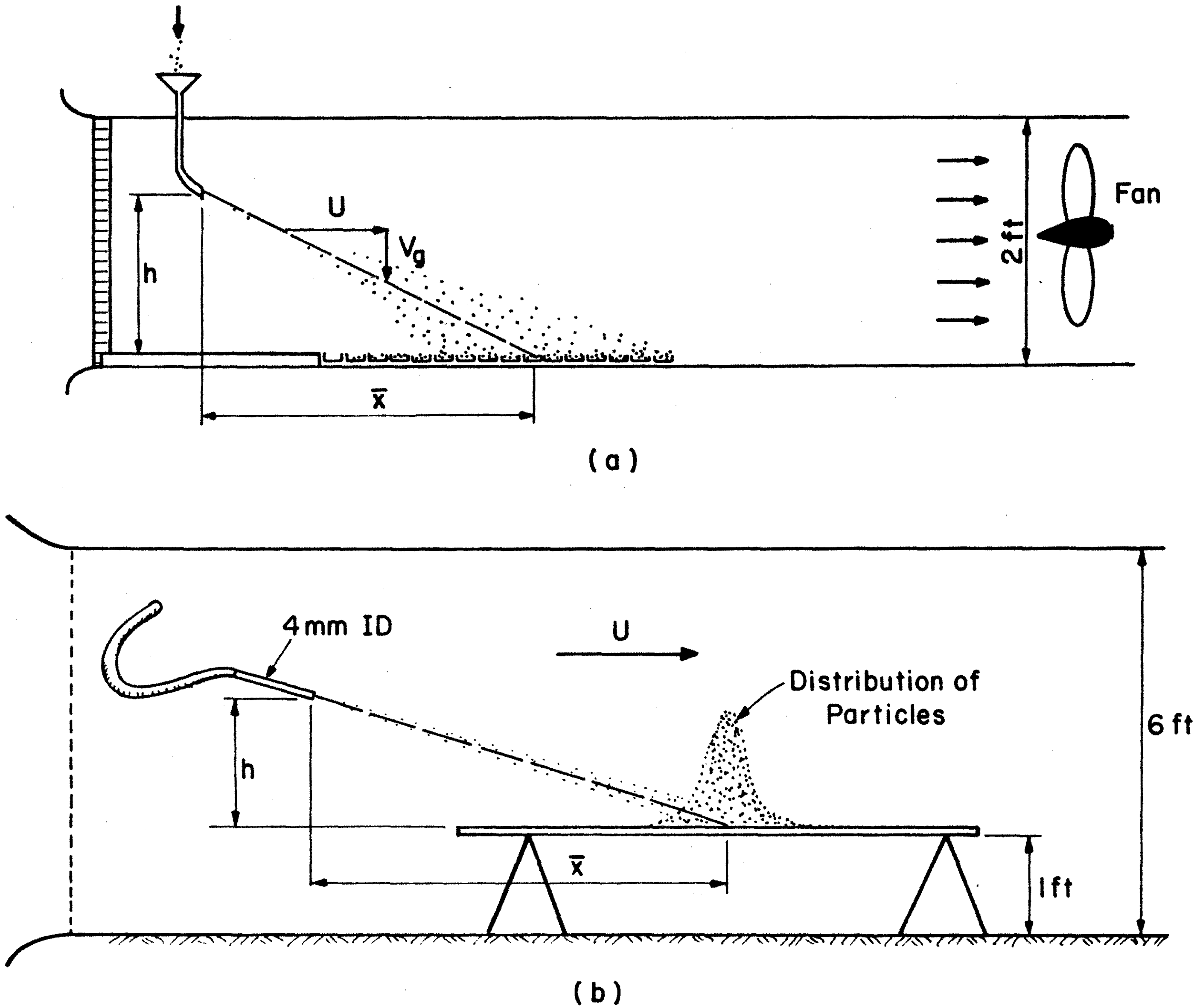

Figure 2. Experimental configurations for (a) sorting the particles and (b) determining their average fall-velocity.

4.3 The Velocity Profile in the Wind Tunnel

Typical mean velocity profiles in the wind tunnel, measured with a calibrated Thermo-system hot wire Model 1050, are shown in Figure 3. We have not used any roughness elements to increase the roughness length of the wind-tunnel floor in order to facilitate the measurement of the particle deposition on the floor. For this reason the velocity profile was relatively flat and is approximately described by Eq. (41) with a power $m = 0.12$.

The wind velocities in the tunnel in the experiments were in the range $U = 3.00 - 7.00$ m/s, where U is the mean velocity at the height of the source.

4.4 Deposition Measurements

Particles were injected into the flow, using the method described earlier, at an angle V_g/U. The average air speed of the air flowing through the tube was U. A few thousand particles were injected at each run.

A light-colored grid was drawn on the black floor of the wind tunnel, which was then covered with a thin layer of machine oil. Particles touching the floor adhered to it and could not move. It was relatively easy to count the number of particles (n) between two lateral lines $x \pm \Delta x/2$ and the number of particles (m) between two longitudinal lines $y(x) \pm \Delta y/2$. The step Δx was 0.5 ft up to $x = 13$ ft and 1 ft after $x = 13$ ft. The step Δy was 0.5 in. up to 12 ft and 1 in. after 12 ft. The mean position $\bar{Y}(x)$ and the standard deviation of the lateral distribution at each distance from the source x, was calculated using the equations

$$\bar{Y} = \Sigma(my)/n$$

and

$$\sigma^2 = \frac{\Sigma\, m(Y_i - \bar{Y})^2}{(n-1)} \quad . \tag{41}$$

Variance of the population $(n\to\infty)$ was assumed as given by the right-hand side of the above equation. The number of particles which had deposited at the very small and very large distances from the source was relatively small. Thus, the estimate of σ is not very accurate. Figure 4 shows two typical lateral distributions of particles which demonstrate this point. Figure 5 shows the measured distributions of $\sigma(x)$ for three identical runs (Runs 1-3). It clearly shows an increased uncertainty in the estimate of σ at small and large distances.

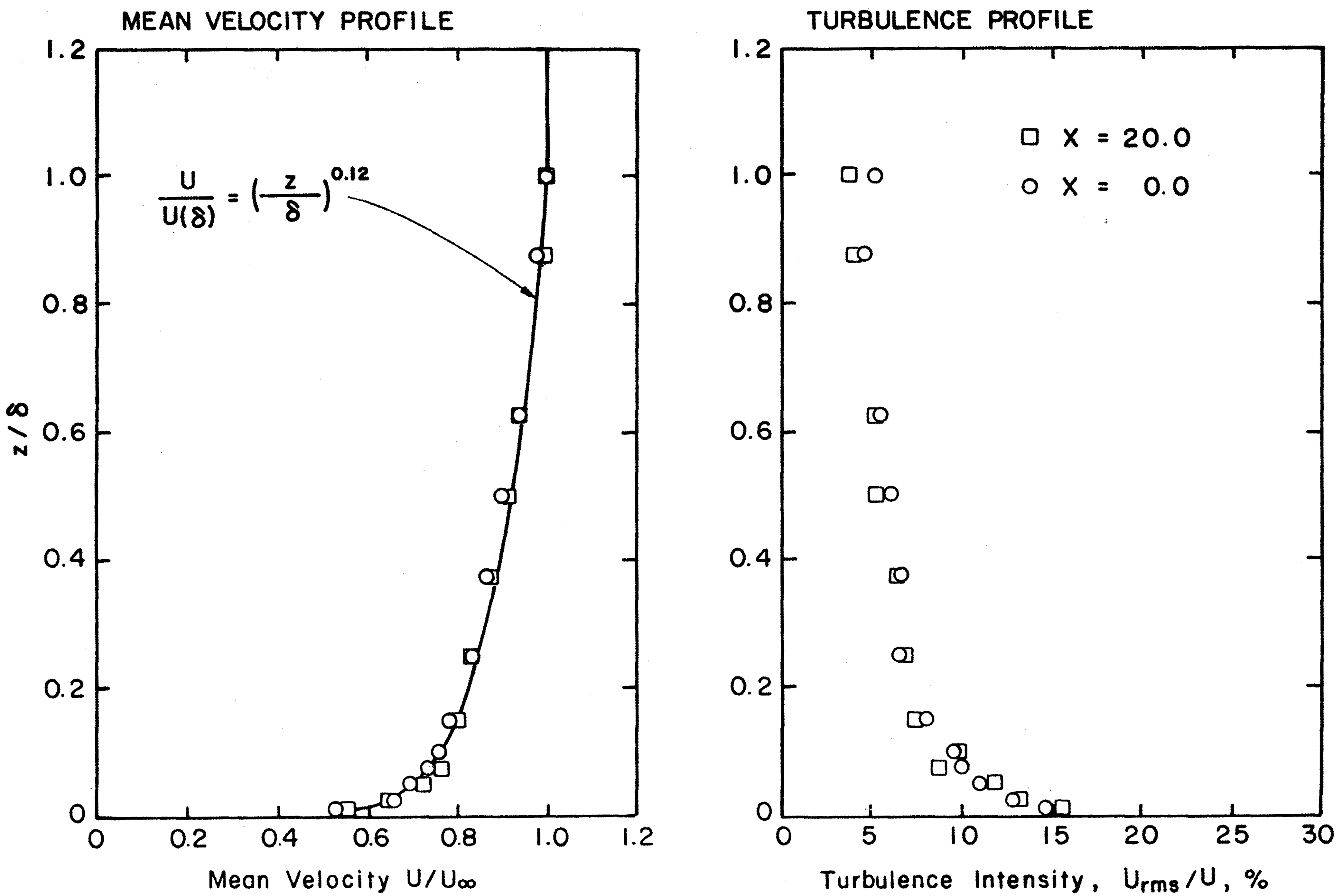

Figure 3. Mean velocity and turbulence profiles in the wind tunnel.

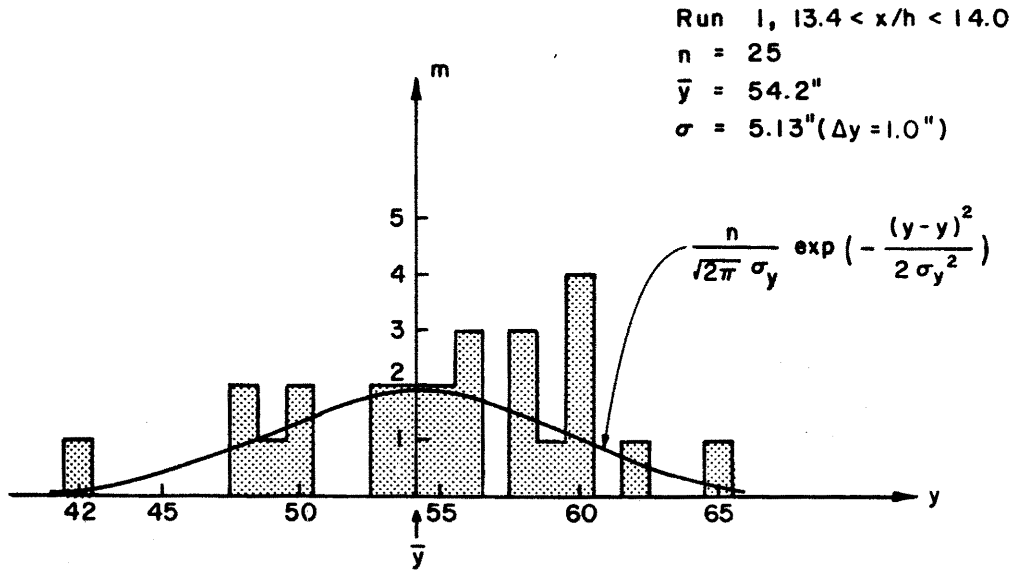

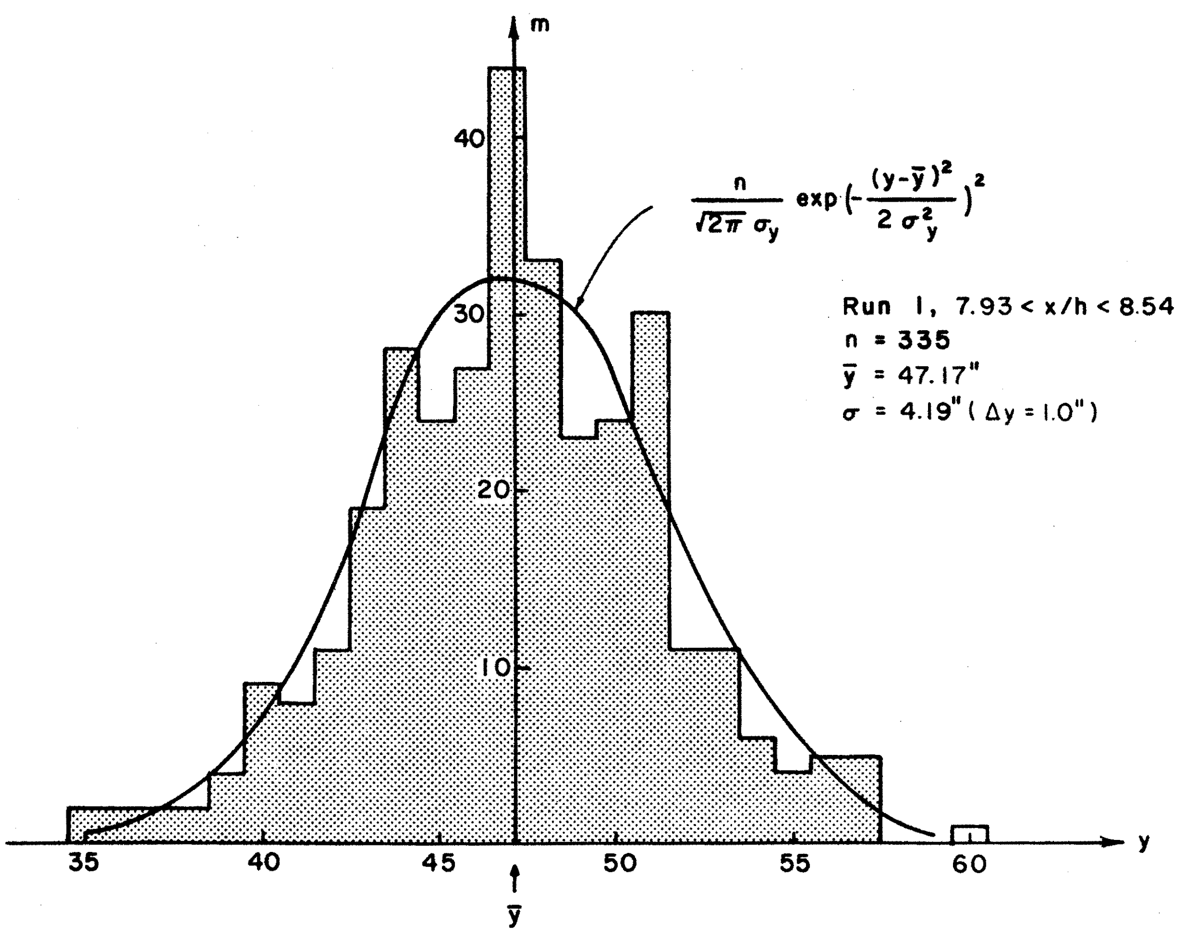

Figure 4. Typical lateral distribution of particles.

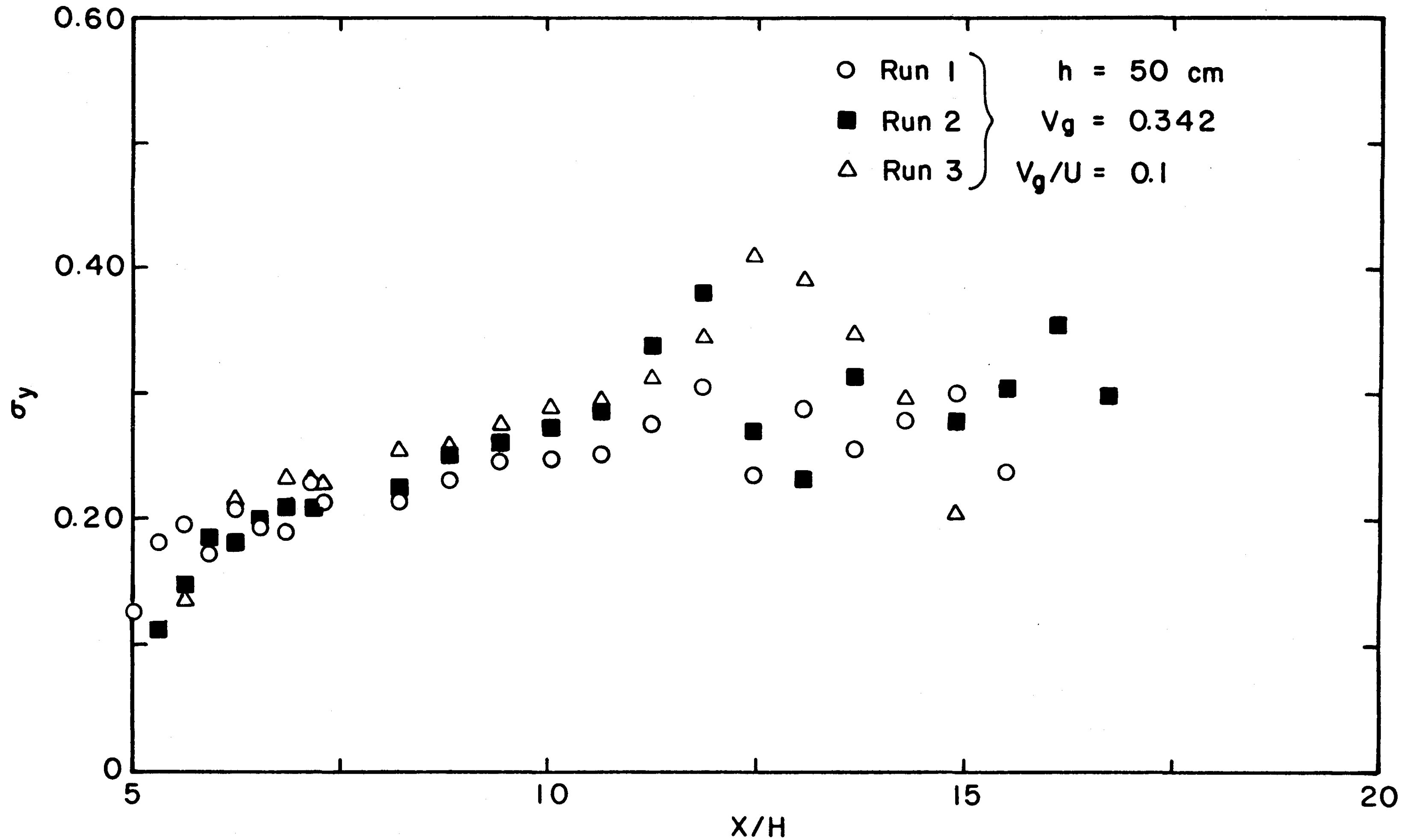

Figure 5. Measured values of $\sigma_y(x^*)$ in three identical runs.

4.5 The Experimental Program

The experimental program was composed of 16 runs, in which the deposition of 6 groups of particles released from 2 heights, at the same dimensionless mean velocity field, was measured.

The mean velocities in these runs were selected to produce five different velocity ratios V_g/U. Note that the mean velocity U is the velocity at the height of the source $z = h$.

The values of the various parameters in each run are given in Table 1. The measured longitudinal distribution of the particles on the floor of the wind tunnel and the values of $\bar{Y}$ and $\sigma_y(x)$ are presented in Table 2.

Table I
The Experimental Program

Run No.	h (m)	V_g m/sec	V_g/U	V_g^2/gh	N
1	0.50	.34	.10	.024	2326
2	0.50	.34	.10	.024	2396
3	0.50	.34	.10	.024	4083
4	0.50	.42	.11	.035	2504
5	0.50	.300	.10	.018	2311
6	0.50	.65	.10	.087	4605
7	0.50	.61	.10	.076	3499
9	0.50	.34	.075	.024	2718
10	0.50	.34	.06	.024	6117
11	0.375	.34	.10	.029	2799
12	0.375	.28	.10	.021	1132
13	0.375	.32	.075	.029	2966
14	0,375	.61	.10	.10	1705
15	0.375	.42	.11	.047	2008
16	0.375	.32	.06	.029	3187
17	0.375	.32	.047	.029	4133

Table 2. The experimental results.*

RUN NO. = 1

H=.500 VG=.342 VG**2/(g*H)= .024
(VG/U)= .100 ΣN=2326

I	X/H	N	SGNO/H	YA/H
1	4.72	3	.1077	2.083
2	5.03	8	.0879	2.165
3	5.33	18	.2713	2.296
4	5.64	28	.3734	2.271
5	5.94	46	.3988	2.216
6	6.25	74	.3490	2.219
7	6.55	94	.4201	2.255
8	6.86	146	.3876	2.315
9	7.16	153	.1895	2.333
10	7.77	322	.2296	2.336
11	8.38	335	.2134	2.396
12	8.99	280	.2144	2.403
13	9.60	224	.2301	2.420
14	10.21	167	.2459	2.478
15	10.82	128	.2479	2.512
16	11.43	84	.2525	2.554
17	12.04	68	.2779	2.626
18	12.65	58	.3073	2.651
19	13.26	32	.2367	2.718
20	13.87	25	.2540	2.753
21	14.48	16	.2606	2.753
22	15.09	9	.2865	2.834

RUN NO. = 2

H=.500 VG=.342 VG**2/(g*H)= .024
(VG/U)= .100 ΣN=2393

I	X/H	N	SGNO/H	YA/H
1	5.33	16	.2352	2.232
2	5.64	31	.3002	2.206
3	5.94	60	.3749	2.210
4	6.25	77	.3678	2.216
5	6.55	127	.4039	2.272
6	6.86	166	.2088	2.277
7	7.16	180	.2008	2.311
8	7.77	311	.2098	2.310
9	8.38	310	.2261	2.355
10	8.99	287	.2504	2.375
11	9.60	246	.2616	2.431
12	10.21	166	.2733	2.485
13	10.82	121	.2860	2.492
14	11.43	77	.3399	2.489
15	12.04	63	.3825	2.530
16	12.65	50	.2723	2.674
17	13.26	21	.2372	2.634
18	13.87	20	.3216	2.720
19	14.48	19	.2789	2.690
20	15.09	11	.2911	2.928
21	15.70	10	.3205	2.774
22	16.31	11	.3708	2.706
23	16.92	3	.3663	2.896

RUN NO. = 3

H=.500 VG=.342 VG**2/(g*H)= .024
(VG/U)= .100 ΣN=4083

I	X/H	N	SGNO/H	YA/H
1	4.72	6	.1692	1.871
2	5.03	9	.2911	2.069
3	5.33	35	.2201	2.069
4	5.64	54	.2794	2.026
5	5.94	85	.3429	2.039
6	6.25	153	.4293	2.032
7	6.55	211	.3998	2.070
8	6.86	229	.2322	2.091
9	7.16	277	.2327	2.106
10	7.77	590	.2271	2.131
11	8.38	635	.2560	2.144
12	8.99	591	.2576	2.177
13	9.60	402	.2753	2.210
14	10.21	312	.2896	2.287
15	10.82	212	.2962	2.304
16	11.43	133	.3145	2.375
17	12.04	123	.3465	2.483
18	12.65	63	.4155	2.485
19	13.26	42	.3962	2.579
20	13.87	37	.3515	2.499
21	14.48	18	.3068	2.560
22	15.09	20	.2108	2.588

RUN NO. = 4

H=.500 VG=.373 VG**2/(g*H)= .023
(VG/U)= .100 ΣN=2504

I	X/H	N	SGNO/H	YA/H
1	5.03	25	.2901	1.957
2	5.33	45	.3475	1.913
3	5.64	72	.3612	1.950
4	5.94	127	.3216	1.980
5	6.25	173	.3795	[illegible]
6	6.55	193	.4131	2.035
7	6.86	240	.2032	2.077
8	7.16	218	.2108	2.094
9	7.77	380	.2012	2.127
10	8.38	296	.2210	2.133
11	8.99	248	.2606	2.167
12	9.60	162	.2611	[illegible]
13	10.21	113	.2596	2.263
14	10.82	77	.2428	2.237
15	11.43	43	.3510	2.401
16	12.04	28	.2982	2.359
17	12.65	17	.4582	2.325
18	13.26	20	.2753	[illegible]
19	13.87	8	.3581	2.502

*VG ≡ V_g; SGNO ≡ σ_y; YA ≡ $\bar{y}$; H ≡ h.

Table 2 (Continued)

RUN NO. = 5

H=.500 VG=.299 VG**2/(g*H)= .018
(VG/U)= .100 ΣN=2311

I	X/H	N	SGNO/H	YA/H
1	5.03	8	.3851	1.943
2	5.33	13	.3358	1.911
3	5.64	33	.3277	1.986
4	5.94	59	.3688	1.989
5	6.25	110	.4013	2.047
6	6.55	113	.3536	2.037
7	6.86	170	.1869	2.085
8	7.16	178	.2134	2.089
9	7.77	406	.2200	2.118
10	8.38	310	.2129	2.203
11	8.99	270	.2271	2.237
12	9.60	165	.2443	2.272
13	10.21	156	.2621	2.325
14	10.82	99	.2570	2.340
15	11.43	72	.2286	2.409
16	12.04	52	.3200	2.430
17	12.65	39	.3150	2.554
18	13.26	19	.3393	2.430
19	13.87	10	.1758	2.530
20	14.48	10	.2281	2.733
21	15.09	7	.1961	2.606

RUN NO. = 6

H=.500 VG=.650 VG**2/(g*H)= .086
(VG/U)= .100 ΣN=4605

I	X/H	N	SGNO/H	YA/H
1	5.94	27	.4105	1.904
2	6.25	43	.4740	1.736
3	6.55	56	.4674	1.877
4	6.86	102	.2596	1.885
5	7.16	108	.2383	1.902
6	7.77	290	.3023	1.852
7	8.38	357	.2591	1.913
8	8.99	408	.2830	1.941
9	9.60	446	.2916	1.939
10	10.21	407	.2931	1.899
11	10.82	383	.3327	1.932
12	11.43	313	.3175	1.972
13	12.04	270	.3419	1.974
14	12.65	241	.3683	2.054
15	13.26	202	.3658	1.957
16	13.87	162	.3769	2.058
17	14.48	139	.3795	2.003
18	15.09	98	.4227	2.007
19	15.70	90	.4155	2.132
20	16.31	74	.4374	2.124
21	16.92	72	.4079	2.004
22	17.53	47	.3632	2.088
23	18.14	40	.4201	2.107
24	18.75	51	.3835	2.214
25	19.36	27	.2840	2.126
26	19.96	26	.3912	2.257
27	20.57	17	.2596	2.113
28	21.18	16	.3348	2.321
29	21.79	10	.3495	2.804
30	22.40	14	.3739	2.526
31	23.01	15	.4440	2.730

RUN NO. = 7

H=.500 VG=.610 VG**2/(g*H)= .076
(VG/U)= .100 ΣN=3499

I	X/H	N	SGNO/H	YA/H
1	5.94	40	.4059	1.895
2	6.25	70	.4211	1.906
3	6.55	59	.4430	1.930
4	6.86	101	.2134	1.925
5	7.16	121	.2637	1.920
6	7.77	286	.2489	1.949
7	8.38	368	.2606	1.983
8	8.99	333	.2459	1.983
9	9.60	346	.2621	1.985
10	10.21	346	.2916	2.034
11	10.82	265	.3084	2.039
12	11.43	214	.2972	2.069
13	12.04	194	.3419	2.132
14	12.65	138	.3038	2.100
15	13.26	123	.3246	2.144
16	13.87	93	.3211	2.131
17	14.48	86	.3114	2.207
18	15.09	64	.3322	2.139
19	15.70	41	.3109	2.220
20	16.31	36	.4496	2.259
21	16.92	27	.2769	2.303
22	17.53	25	.3033	2.233
23	18.14	21	.3759	2.342
24	18.75	19	.3835	2.227

RUN NO. = 9

H=.500 VG=.342 VG**2/(g*H)= .024
(VG/U)= .075 ΣN=2718

I	X/H	N	SGNO/H	YA/H
1	5.33	1	0.000	1.092
2	5.64	13	0.000	1.092
3	5.94	17	.3764	1.851
4	6.25	35	.3048	1.938
5	6.55	30	.3896	2.009
6	6.86	33	.2393	2.047
7	7.16	42	.2479	2.004
8	7.77	110	.2098	2.068
9	8.38	150	.2565	2.085
10	8.99	218	.2860	2.156
11	9.60	209	.2804	2.179
12	10.21	204	.2758	2.218
13	10.82	215	.3150	2.232
14	11.43	170	.3246	2.270
15	12.04	186	.2835	2.334
16	12.65	165	.3419	2.319
17	13.26	131	.3048	2.373
18	13.87	125	.3170	2.421
19	14.48	85	.4354	2.486
20	15.09	96	.2926	2.481
21	15.70	56	.3683	2.537
22	16.31	68	.4039	2.475
23	16.92	70	.3820	2.477
24	17.53	45	.3907	2.450
25	18.14	42	.3734	2.593
26	18.75	30	.3404	2.620
27	19.36	35	.4354	2.627
28	19.96	24	.3226	2.718
29	20.57	15	0.000	0.000
30	21.18	16	0.000	0.000
31	21.79	11	0.000	0.000
32	22.40	11	0.000	0.000
33	23.01	12	0.000	0.000
34	23.62	9	0.000	0.000
35	24.23	10	0.000	0.000
36	24.84	13	0.000	0.000
37	25.45	7	0.000	0.000
38	26.06	9	0.000	0.000

Table 2 (Continued)

RUN NO. = 10

H=.500 VG=.342 VG**2/(g*H)= .024
(VG/U)= .060 ΣN=6117

I	X/H	N	SGNO/H	YA/H
1	6.55	5	0.000	1.092
2	6.86	5	0.000	0.000
3	7.16	15	0.000	0.000
4	7.77	33	.2662	1.955
5	8.38	72	.2438	2.039
6	8.99	101	.2865	2.089
7	9.60	183	.2530	2.092
8	10.21	197	.2596	2.129
9	10.82	248	.2819	2.133
10	11.43	294	.3094	2.159
11	12.04	284	.3207	2.216
12	12.65	310	.3368	2.222
13	13.26	335	.3368	2.233
14	13.87	322	.3561	2.226
15	14.48	289	.3729	2.297
16	15.09	284	.3759	2.325
17	15.70	293	.3378	2.304
18	16.31	258	.3957	2.314
19	16.92	247	.3749	2.385
20	17.53	218	.3962	2.368
21	18.14	227	.3988	2.397
22	18.75	199	.4145	2.386
23	19.36	164	.4298	2.509
24	19.96	175	.4145	2.478
25	20.57	165	.4171	2.475
26	21.18	138	.4450	2.460
27	21.79	137	.4836	2.911
28	22.40	108	.3749	2.900
29	23.01	90	.5080	2.869
30	23.62	90	.4145	2.928
31	24.23	89	.4267	3.048
32	24.84	73	.4907	2.965
33	25.45	47	.4592	2.873
34	26.06	69	.4115	2.947
35	26.67	64	.4592	3.075
36	27.28	42	.4074	3.092
37	27.89	42	.4440	2.997
38	28.50	48	.4491	3.033
39	29.11	47	.4674	3.119
40	29.72	20	0.000	0.000
41	30.33	42	0.000	0.000
42	30.94	35	0.000	0.000
43	31.55	29	0.000	0.000
44	32.16	23	0.000	0.000
45	32.77	25	0.000	0.000
46	33.38	13	0.000	0.000
47	33.99	18	0.000	0.000

RUN NO. = 11

H=.375 VG=.324 VG**2/(g*H)= .029
(VG/U)= .100 ΣN=2799

I	X/H	N	SGNO/H	YA/H
1	4.27	2	0.000	1.456
2	4.67	4	0.000	1.456
3	5.08	25	.2323	2.646
4	5.49	59	.3509	2.707
5	5.89	91	.4348	2.734
6	6.30	168	.4525	2.751
7	6.71	171	.4897	2.795
8	7.11	242	.5195	2.823
9	7.52	237	.5080	2.852
10	7.92	236	.4856	2.842
11	8.33	212	.5127	2.897
12	8.74	206	.5222	2.937
13	9.14	197	.2933	2.973
14	9.55	149	.2621	2.982
15	10.36	241	.2805	3.045
16	11.18	183	.2730	3.181
17	11.99	125	.3007	3.234
18	12.80	74	.3454	3.269
19	13.61	47	.3549	3.300
20	14.43	46	.3563	3.274
21	15.24	19	.3102	3.379
22	16.05	21	.5683	3.419
23	16.87	12	0.000	0.000
24	17.68	9	0.000	0.000
25	18.49	9	0.000	0.000
26	19.30	5	0.000	0.000
27	20.12	4	0.000	0.000
28	20.93	5	0.000	0.000

RUN NO. = 12

H=.375 VG=.281 VG**2/(g*H)= .022
(VG/U)= .100 ΣN=1132

I	X/H	N	SGNO/H	YA/H
1	4.67	3	0.000	1.456
2	5.08	14	0.000	1.456
3	5.49	20	0.000	1.456
4	5.89	35	.4247	2.644
5	6.30	64	.4139	2.726
6	6.71	63	.4267	2.813
7	7.11	89	.4748	2.835
8	7.52	97	.4619	2.931
9	7.92	96	.4938	2.936
10	8.33	104	.6265	2.918
11	8.74	99	.5392	2.973
12	9.14	84	.3265	2.980
13	9.55	60	.3258	3.131
14	10.36	102	.3421	3.104
15	11.18	62	.3156	3.253
16	11.99	49	.4328	3.247
17	12.80	34	.4125	3.343
18	13.61	23	.4965	3.319
19	14.43	23	0.000	0.000
20	15.24	11	0.000	0.000

RUN NO. = 13

H=.375 VG=.324 VG**2/(g*H)= .029
(VG/U)= .075 ΣN=2966

I	X/H	N	SGNO/H	YA/H
1	5.49	3	0.000	1.456
2	5.89	5	0.000	1.456
3	6.30	16	0.000	1.456
4	6.71	26	.3685	2.728
5	7.11	54	.3962	2.730
6	7.52	76	.4599	2.755
7	7.92	86	.4755	2.749
8	8.33	128	.4647 @	2.778
9	8.74	122	.4890	2.789
10	9.14	152	.2377	2.890
11	9.55	186	.2750	2.904
12	10.36	329	.2865	2.952
13	11.18	350	.3007	2.994
14	11.99	280	.2973	3.062
15	12.80	231	.5635	2.958
16	13.61	201	.3610	3.166
17	14.43	155	.4037	3.200
18	15.24	120	.3597	3.369
19	16.05	94	.4193	3.388
20	16.87	77	.4267	3.469
21	17.68	70	.4443	3.436
22	18.49	44	.4416	3.398
23	19.30	43	.4470	3.502
24	20.12	37	.4260	3.685
25	20.93	21	.4396	3.557
26	21.74	19	.3068	3.757
27	22.56	15	0.000	0.000
28	23.37	17	0.000	0.000
29	24.18	7	0.000	0.000
30	24.99	2	0.000	0.000

Table 2 (Continued)

RUN NO. = 14

H=.375 VG=.609 VG**2/(g*H)= .101
(VG/U)= .100 ΣN=1705

I	X/H	N	SGNO/H	YA/H
1	4.67	2	0.000	1.456
2	5.08	16	0.000	1.456
3	5.49	23	0.000	1.456
4	5.89	38	.3976	2.463
5	6.30	40	.4328	2.471
6	6.71	54	.4951	2.435
7	7.11	65	.5066	2.513
8	7.52	91	.5480	2.507
9	7.52	115	.5608	2.552
10	8.33	96	.6299	2.505
11	8.74	101	.6455	2.598
12	9.14	116	.3969	2.615
13	9.55	104	.3549	2.682
14	10.36	196	.3583	2.703
15	11.18	148	.4098	2.743
16	11.99	116	.3820	2.743
17	12.80	90	.3759	2.804
18	13.61	60	.4389	2.852
19	14.43	55	.4389	2.892
20	15.24	48	.3969	3.001
21	16.05	40	.4233	3.109
22	16.87	29	.4606	3.109
23	17.68	14	.5114	3.102
24	18.49	15	0.000	0.000
25	19.30	14	0.000	0.000
26	20.12	10	0.000	0.000
27	20.93	7	0.000	0.000
28	21.74	2	0.000	0.000

RUN NO. = 15

H=.375 VG=.373 VG**2/(g*H)= .038
(VG/U)= .100 ΣN=2008

I	X/H	N	SGNO/H	YA/H
1	4.27	2	0.000	1.456
2	4.67	9	0.000	1.456
3	5.08	31	0.000	1.456
4	5.49	65	.3725	2.643
5	5.89	116	.3651	2.664
6	6.30	136	.4355	2.691
7	6.71	163	.5053	2.703
8	7.11	219	.4958	2.739
9	7.52	207	.4870	2.764
10	7.92	184	.5459	2.822
11	8.33	155	.5148	2.840
12	8.74	143	.5588	2.905
13	9.14	122	.3055	2.954
14	9.55	85	.2818	2.936
15	10.36	137	.2973	2.988
16	11.18	92	.3488	3.070
17	11.99	41	.2865	3.146
18	12.80	29	.4362	3.139
19	13.61	28	.4782	3.196
20	14.43	13	0.000	0.000
21	15.24	10	0.000	0.000
22	16.05	5	0.000	0.000
23	16.87	4	0.000	0.000
24	17.68	2	0.000	0.000

RUN NO. = 16

H=.375 VG=.324 VG**2/(g*H)= .029
(VG/U)= .060 ΣN=3187

I	X/H	N	SGNO/H	YA/H
1	6.30	4	0.000	1.456
2	6.71	4	0.000	1.456
3	7.11	6	0.000	1.456
4	7.52	82	.4409	2.313
5	7.92	38	.6252	2.781
6	8.33	35	.4240	2.988
7	8.74	52	.5751	2.965
8	9.14	51	.3624	2.717
9	9.55	67	.3319	2.766
10	10.36	198	.4227	3.352
11	11.18	223	.3468	2.801
12	11.99	221	.3901	2.830
13	12.80	217	.4159	2.890
14	13.61	232	.3793	2.933
15	14.43	175	.4125	3.020
16	15.24	200	.4477	3.069
17	16.05	155	.4823	3.147
18	16.87	117	.4118	3.213
19	17.68	138	.3868	3.192
20	18.49	173	.3915	3.221
21	19.30	101	.5195	3.221
22	20.12	86	.4999	3.303
23	20.93	69	.4890	3.306
24	21.74	65	.4409	3.251
25	22.56	79	.5337	3.311
26	23.37	53	.5317	3.430
27	24.18	53	.4240	3.472
28	24.99	41	0.000	0.000
29	25.81	49	0.000	0.000
30	26.62	37	0.000	0.000
31	27.43	35	0.000	0.000
32	28.25	29	0.000	0.000
33	29.06	25	0.000	0.000
34	29.87	23	0.000	0.000
35	30.68	17	0.000	0.000
36	31.50	15	0.000	0.000
37	32.31	14	0.000	0.000
38	33.12	8	0.000	0.000

RUN NO. = 17

H=.375 VG=.324 VG**2/(g*H)= .029
(VG/U)= .047 ΣN=4133

I	X/H	N	SGNO/H	YA/H
1	7.11	4	0.000	1.456
2	7.52	7	0.000	1.456
3	7.92	2	0.000	1.456
4	8.33	7	0.000	1.456
5	8.74	8	0.000	1.456
6	9.14	17	.2845	2.703
7	9.55	26	.4199	2.642
8	10.36	57	.4159	2.452
9	11.18	71	.3515	2.526
10	11.99	94	.4152	2.479
11	12.80	124	.3739	2.533
12	13.61	124	.4443	2.581
13	14.43	148	.4619	2.526
14	15.24	184	.4450	2.543
15	16.05	183	.4301	2.600
16	16.87	183	.5236	2.568
17	17.68	198	.4938	2.438
18	18.49	191	.5297	2.540
19	19.30	176	.5121	2.591
20	20.12	155	.5791	2.487
21	20.93	167	.5988	2.684
22	21.74	175	.6272	2.735
23	22.56	151	.6550	2.705
24	23.37	135	.6787	2.561
25	24.18	160	.6868	2.528
26	24.99	145	.6496	2.478
27	25.81	114	.6658	2.447
28	26.62	111	.7552	2.569
29	27.43	105	.7383	2.661
30	28.25	68	.7396	2.517
31	29.06	104	.7938	2.937
32	29.87	81	.7735	3.323
33	30.68	65	.8873	3.026
34	31.50	73	.7627	3.020
35	32.31	69	.6123	3.174
36	33.12	61	.6529	3.331
37	33.93	62	.8453	3.159
38	34.75	47	.8900	3.297
39	35.56	77	.9442	3.236
40	36.37	51	.7315	3.549
41	37.19	53	0.000	0.000
42	38.00	53	0.000	0.000
43	38.81	50	0.000	0.000

5 ANALYSIS OF THE RESULTS

5.1 The Analytical Model

The very simple analytical expression for the probability of deposition, which gives the relative cross-wind concentration on the ground per unit length, makes it easy to evaluate the effect of the various variables on the deposition pattern. Of course, the restrictions of the model should be recalled before using this expression.

The dimensionless distribution $P(x^*)$ can be written as

$$P(x^*) = \frac{nh}{Ndx} = \frac{(1+m)}{(2\pi)^{\frac{1}{2}}} \frac{V_g}{U} \frac{h}{\sigma_z} \exp\left[- \frac{\left(1 - \frac{(1+m)V_g x}{Uh}\right)^2}{2(\sigma_z/h)^2} \right] \quad . \qquad (42)$$

Since the variation of the first factor in this equation is relatively slow, the position of maximum deposition, X_{max}, is primarily determined by the second factor and is expected to be at

$$\frac{X_{max}}{h} = e \cdot \frac{U}{(1+m)V_g} \qquad (43)$$

where e is a coefficient which is smaller than 1.

Figure 6 shows the dependence of X^*_{max} on the relative fall velocity V_g/U, according to Eq. (42). It also shows the approximate solution (43), with $e = 1$. One sees that e varies between 0.77 to 0.96 in the range $0.02 < V_g/U < 0.1$.

The maximum deposition rate, at that point, is approximately given by

$$P(x^*)_{max} = \frac{(1+m)}{(2\pi)^{\frac{1}{2}}} \frac{V_g}{U\, \sigma^*(x^*_{max})} \qquad (44)$$

Using Eq. (44), one finds that

$$P(x^*)_{max} = \frac{(1+m)^{1+b}}{k\sqrt{2\pi}} \left(\frac{V_g}{U}\right)^{1+b} \left(\frac{h}{\delta}\right)^{(1-b)} \qquad (45)$$

Figure 7 shows the exact theoretical solution for $P(x^*)_{max}$ for $h/\delta = 0.5$. It also shows that the approximate solution (Eq. (45)) deviates from the exact solution by a small fraction only. Figure 8 shows the dimensionless distribution $P(x^*)$ for three velocity ratios

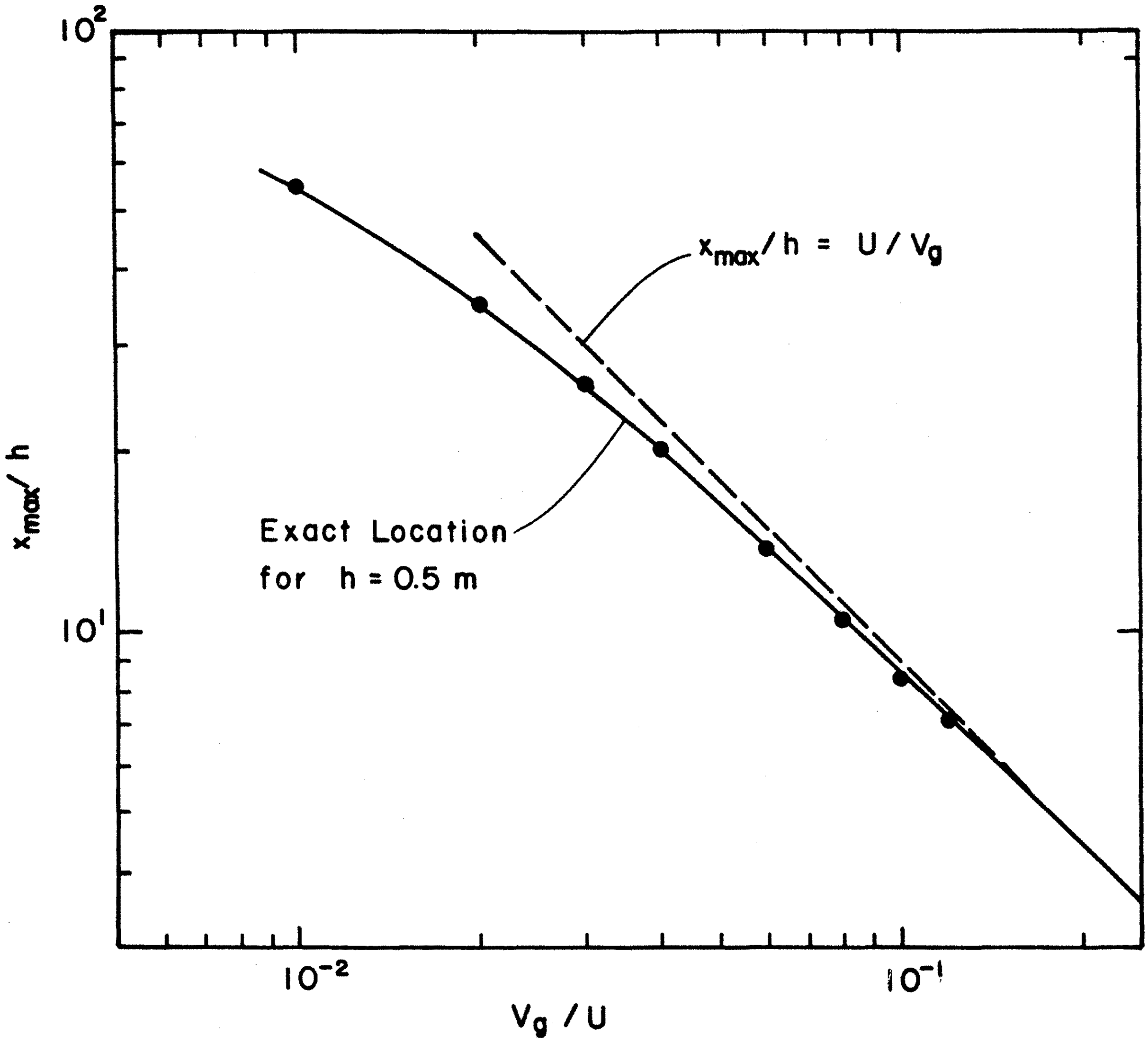

Figure 6. The dependence of the position of maximum deposition x^*_{max} on V_g/U.

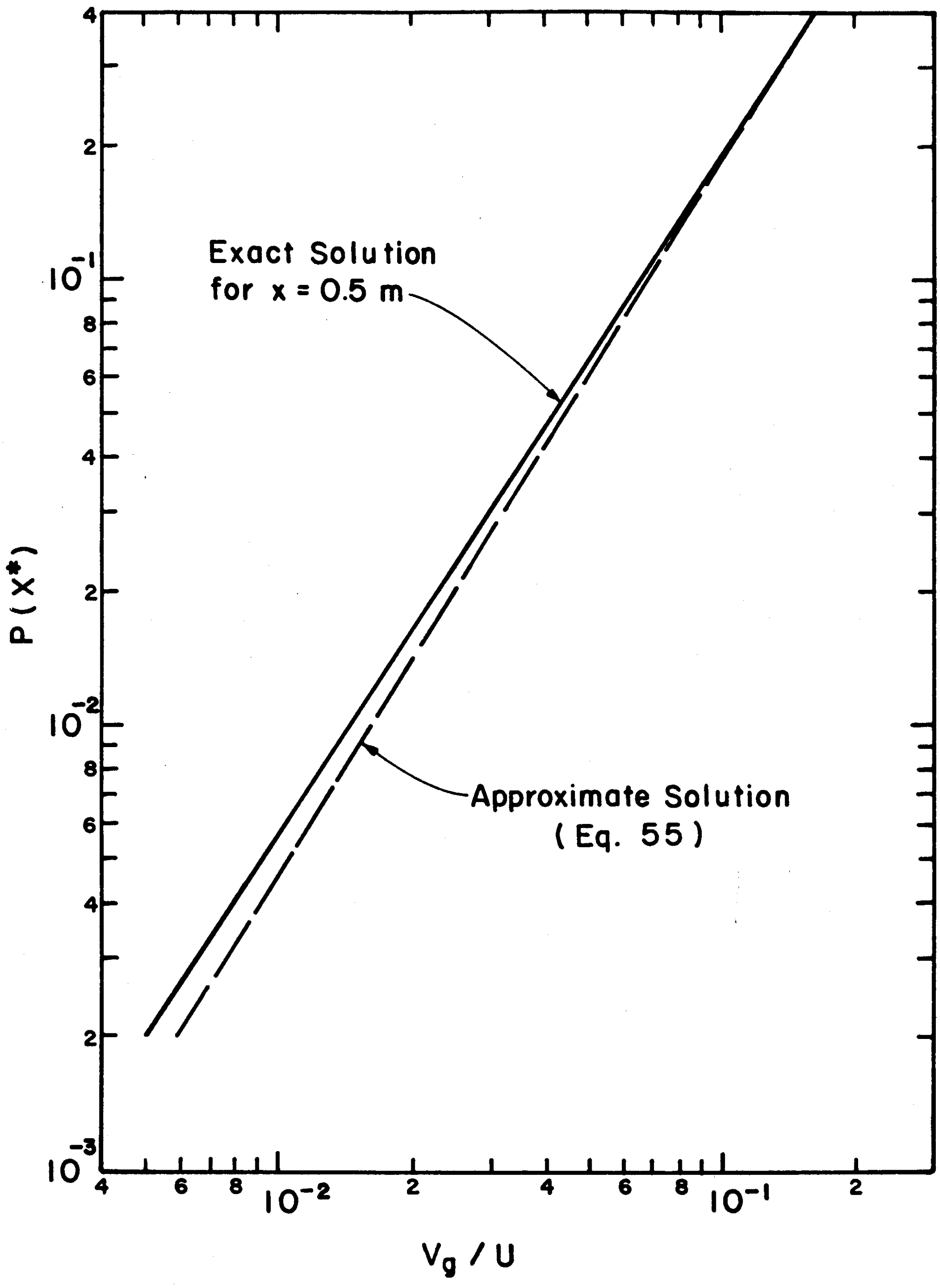

Figure 7. The dependence of $P(x^*)_{max}$ on V_g/U.

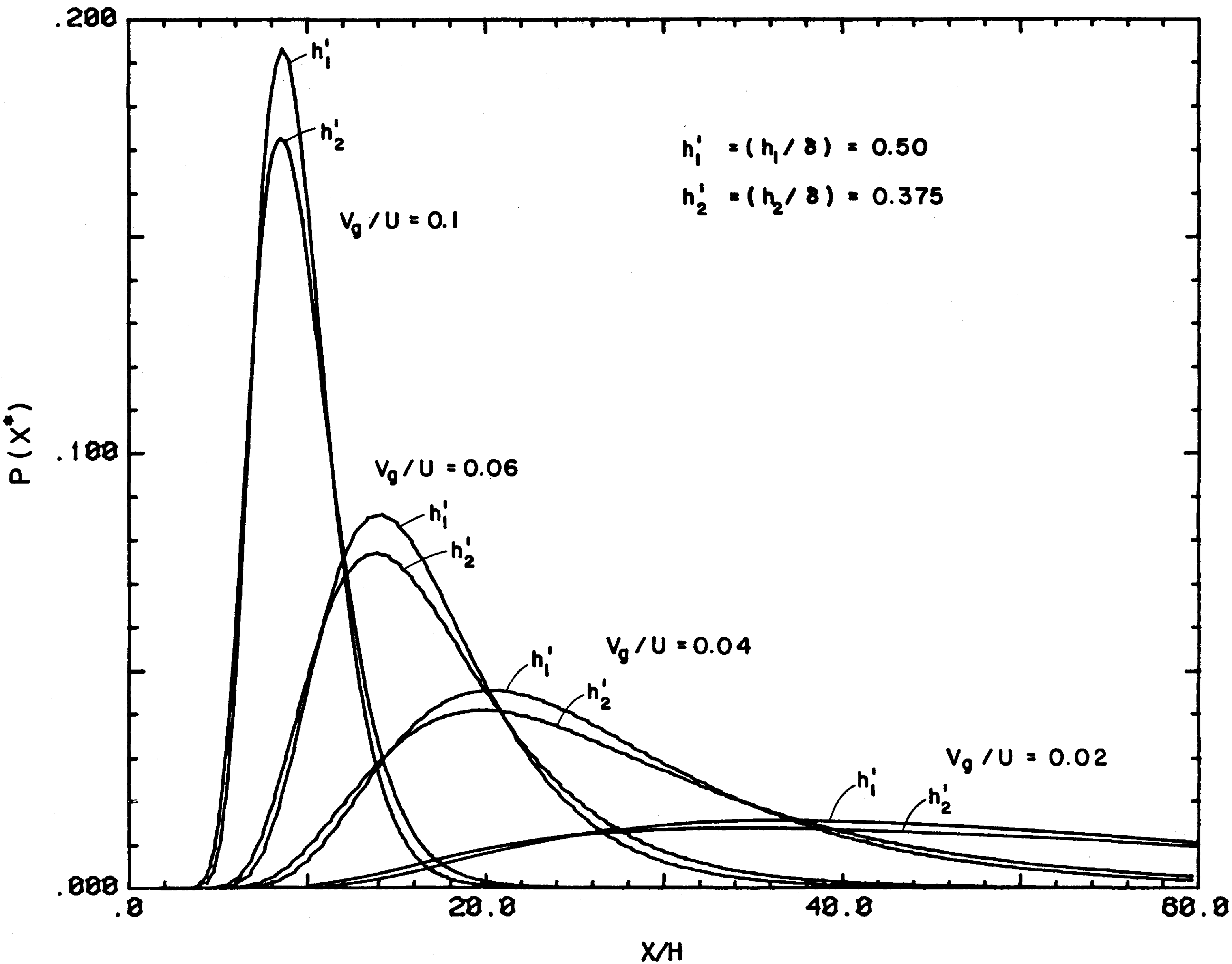

Figure 8. The dimensionless distribution $P(x^*)$ for different velocity ratios and different source heights.

and two values of h. The figure clearly demonstrates that the velocity ratio is the most significant parameter that affects the longitudinal dimensionless probability of the particle distribution. The function $P(x^*)$ data for h = 0.5 m is also plotted in Figure 9, using log-log coordinates.

5.2 The Measured Longitudinal Deposition

Before comparing the measured longitudinal deposition of the particles with the model (Eq. (35)), attention should be given to the effect of possible errors in the estimated average values of V_g/U for each group of particles as well as to the effect of the distribution of V_g/U in each group.

We have seen earlier that the position of the maximum concentration x^*_{max} is proportional to hU/V_g. Thus, the error in x^*_{max} is proportional to values of the errors in estimating these parameters. The maximum of $P(x^*)$ is proportional to $(V_g/U)^{1.6}$ and thus a 10% error in V_g/U will produce a 16% error in $P(x^*)_{max}$.

Fractional errors in estimating V_g/U might, however, cause dramatic changes in the value of $P(x^*)$ at particular locations x^*, smaller or larger than x^*_{max} as demonstrated in Figure 10. Thus, the agreement between the experimental and theoretical results should be evaluated by the differences in x^*_{max} and $P(x^*)_{max}$ and by the general shape of the distribution $P(x^*)$ and not by the differences between the values of $P(x^*)$ at small and large distances.

We have mentioned earlier that the distribution of the velocity ratio of particles within each group was much larger for particles with large fall velocities. To demonstrate the effect of the distribution of V_g/U within each group we have plotted in Figure 11 the theoretical distributions for three groups, each composed of two mono-dispersed subgroups with fall velocities $V_g/U = 0.1\,(1 \pm \varepsilon)$; $\varepsilon = 0$, 0.1 and 0.2. One clearly sees that while the maximum concentration and its location decrease with the nonuniformity of the particles, the small concentrations at very small and very large distances increase with increasing nonuniformity.

The measured relative dimensionless cross-wind concentrations of the particles on the wind-tunnel floor, $C^y(x^*)$, which are equivalent to the deposition longitudinal probability $P(x^*)$ are presented in Figures 12-22 together with the theoretical predictions of the model, assuming that all the particles in each group have the same fall velocity and that the value of σ is given by Eq. (40).

Figure 12 presents the measurements from Runs 1, 2, 3, and 5, which had the same estimated mean relative fall velocity $V_g/U = 0.10$. It is noted that Runs 1, 2, and 3, in which the same particles were used, gave almost identical longitudinal concentration distributions. The location

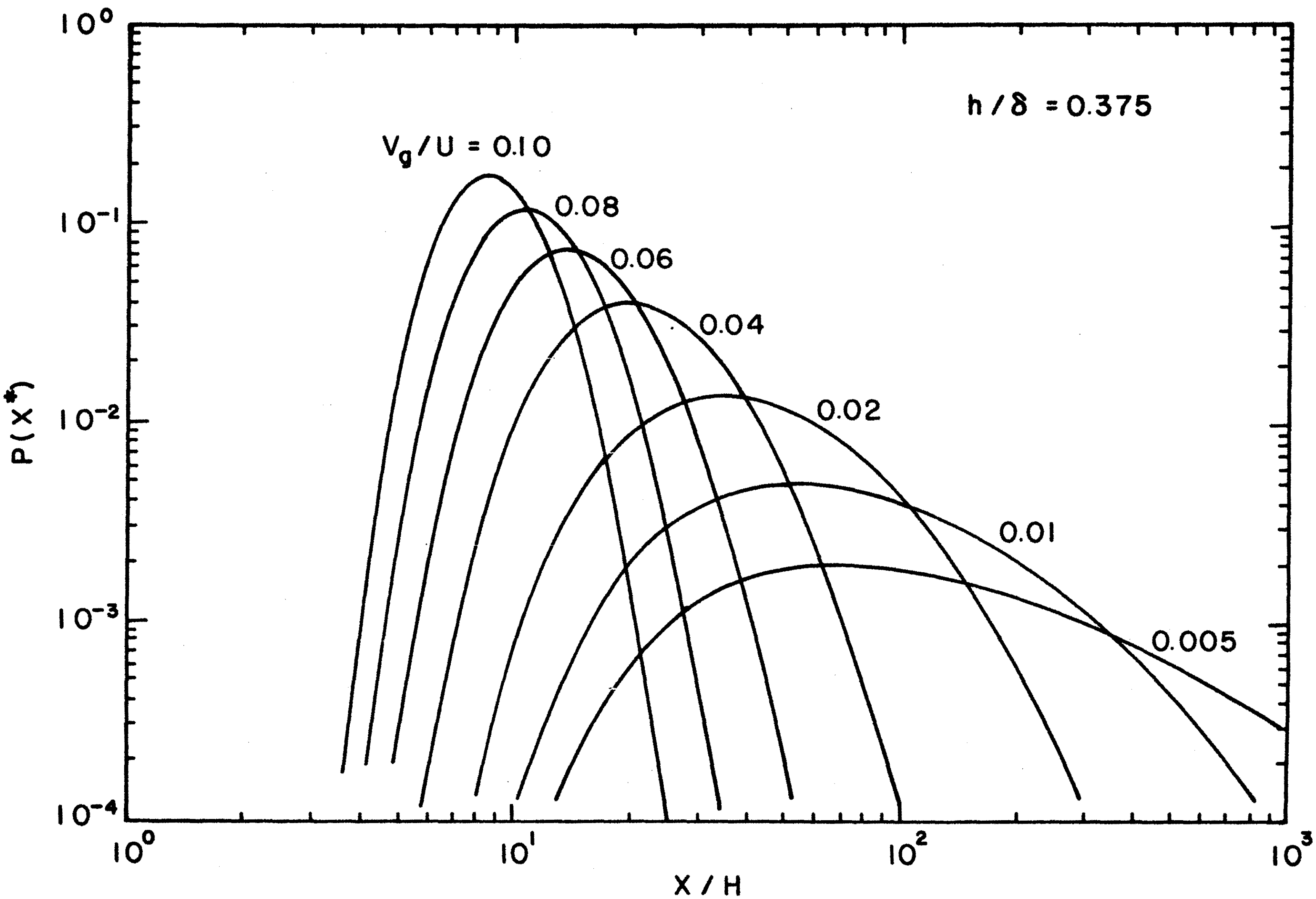

Figure 9. The effect of V_g/U on the longitudinal deposition of particles (Eq. (53)).

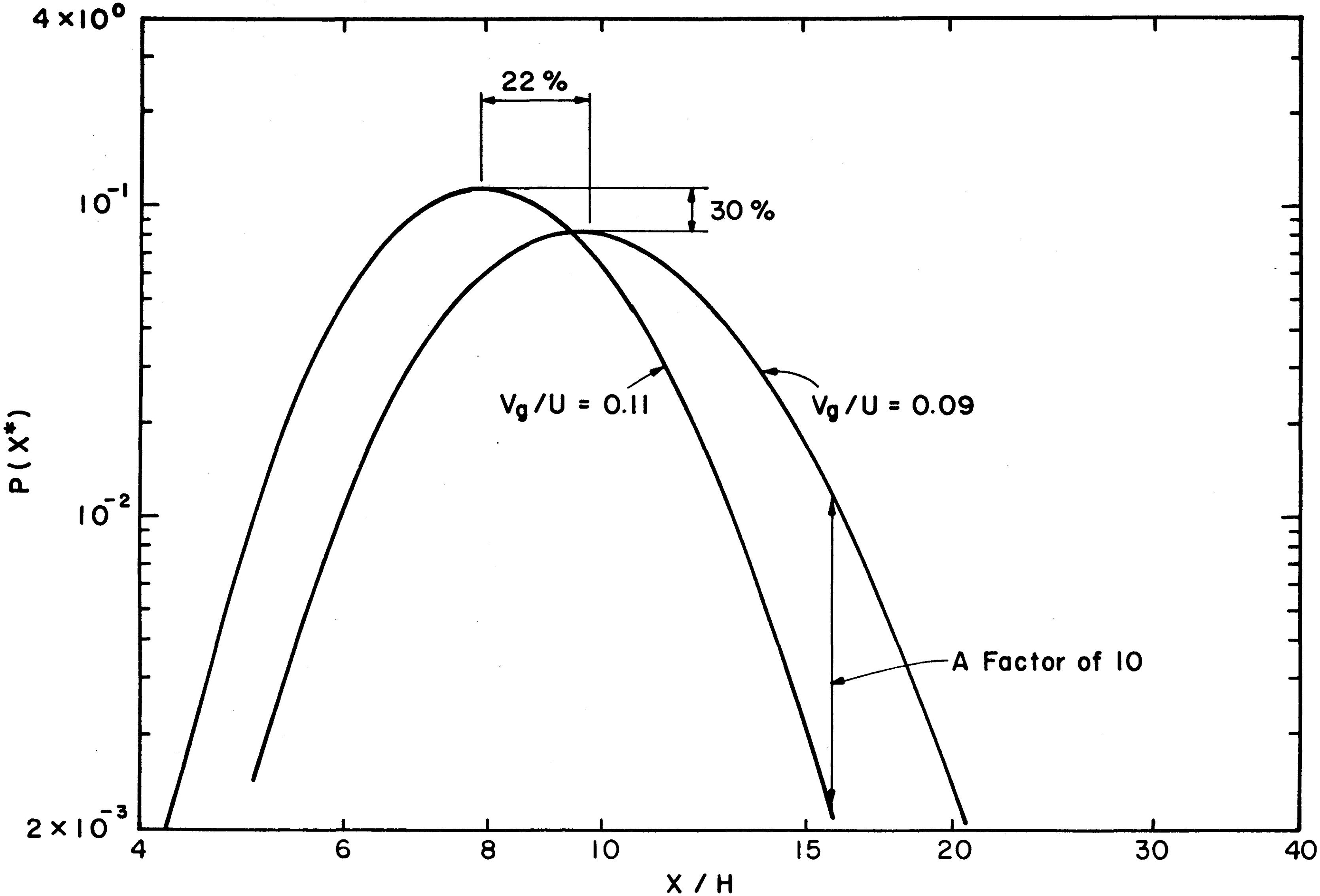

Figure 10. The effect of small changes in V_g/U on $P(x^*)$.

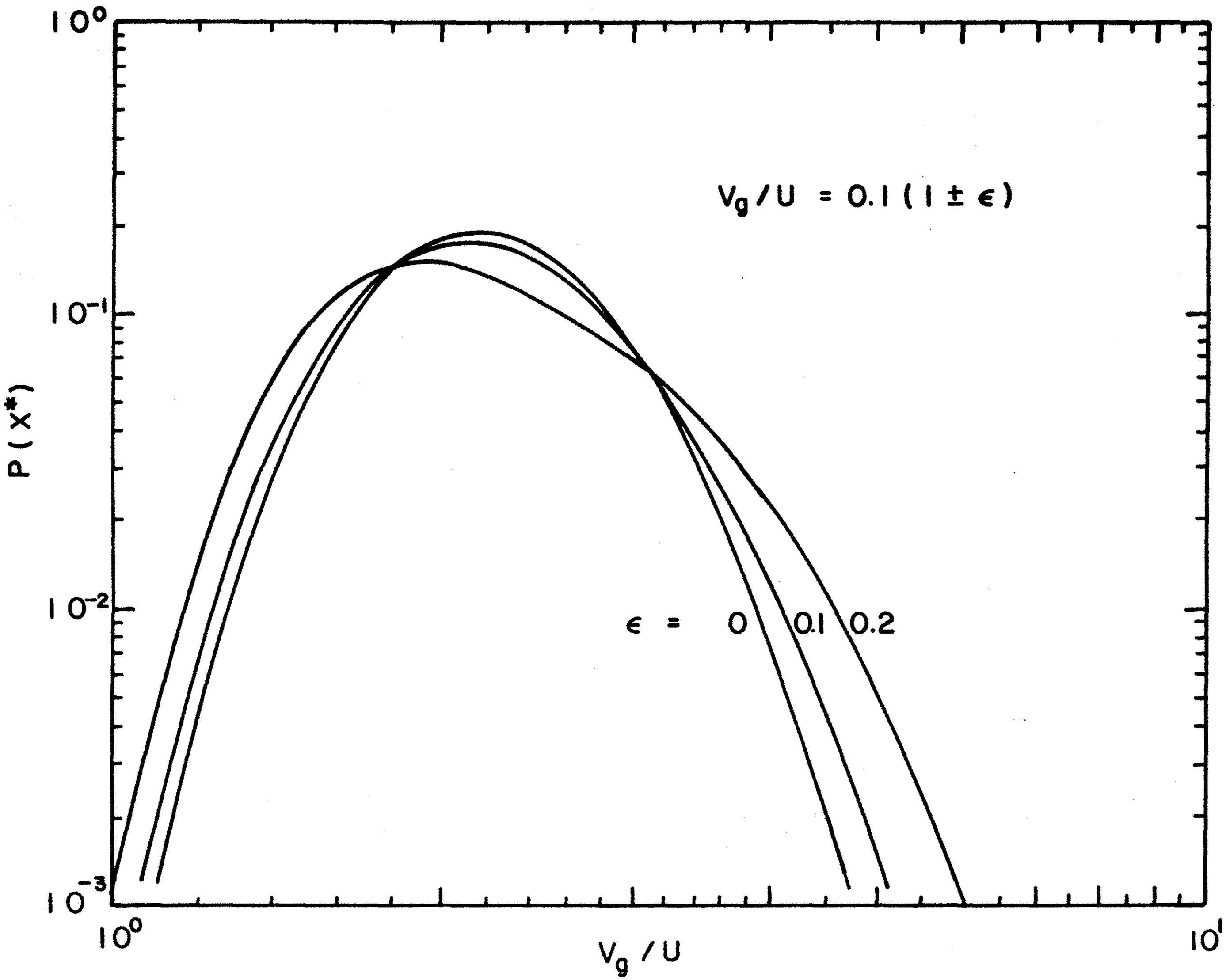

Figure 11. The combined distributions of two equal mono-dispersed groups of particles with fall velocities $V_g/U = 0.1(1 \pm \varepsilon)$.

Figure 12

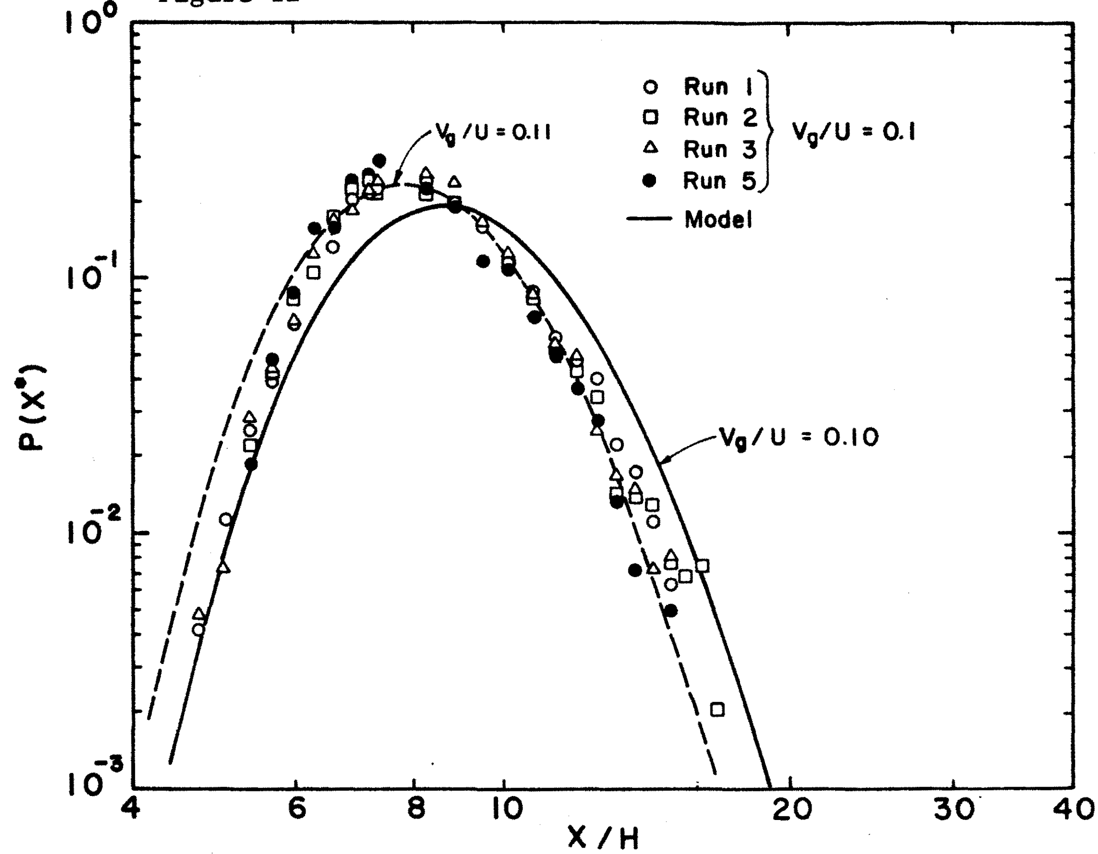

Figure 13

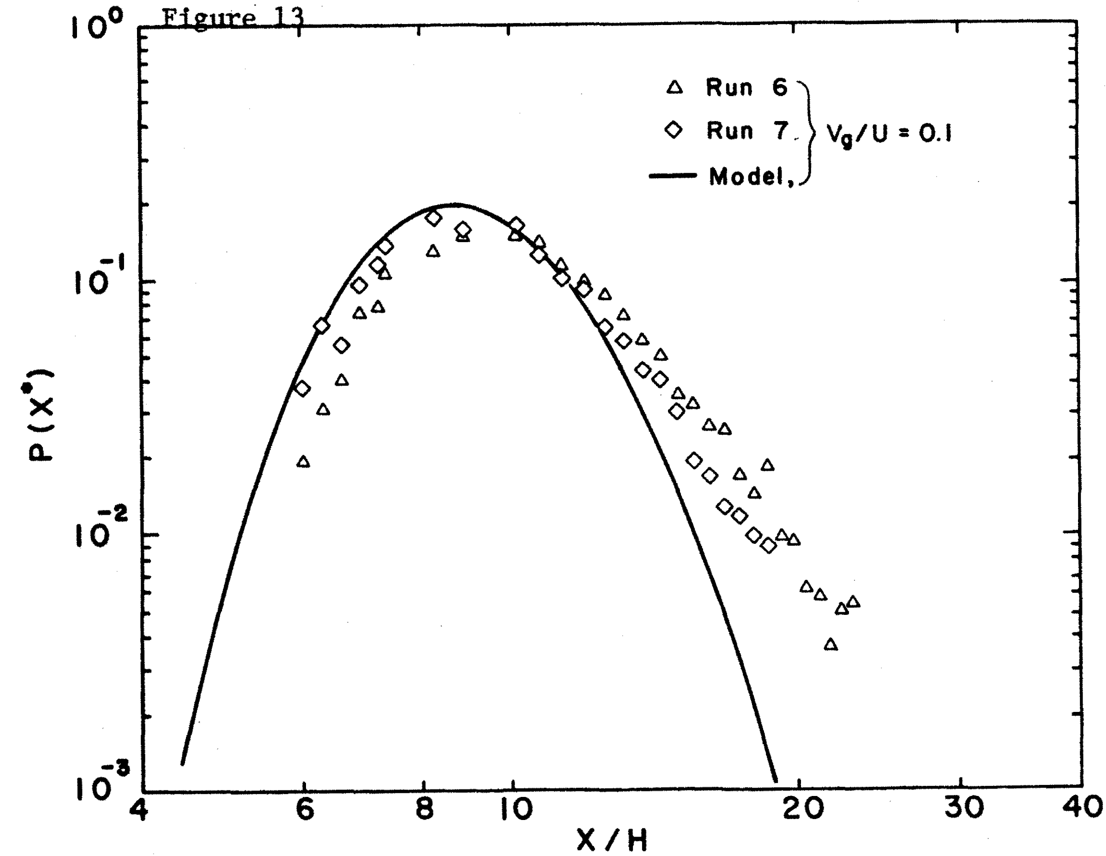

Figures 12-13. The longitudinal deposition of the particles ($V_g/V = 0.1$, $h/\delta = 0.5$).

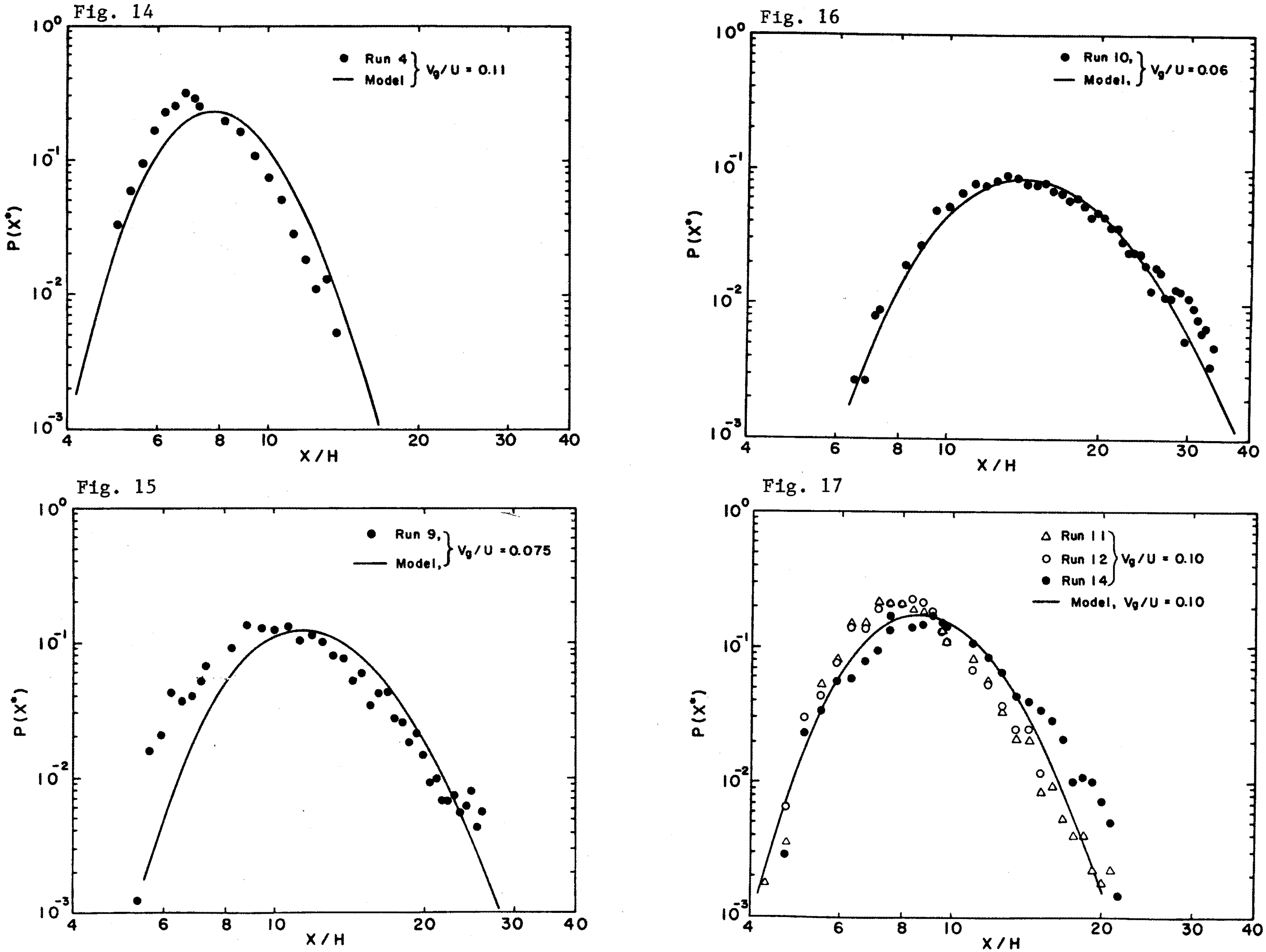

Figures 14-17. The longitudinal deposition of particles $P(x^*)$.

Fig. 18

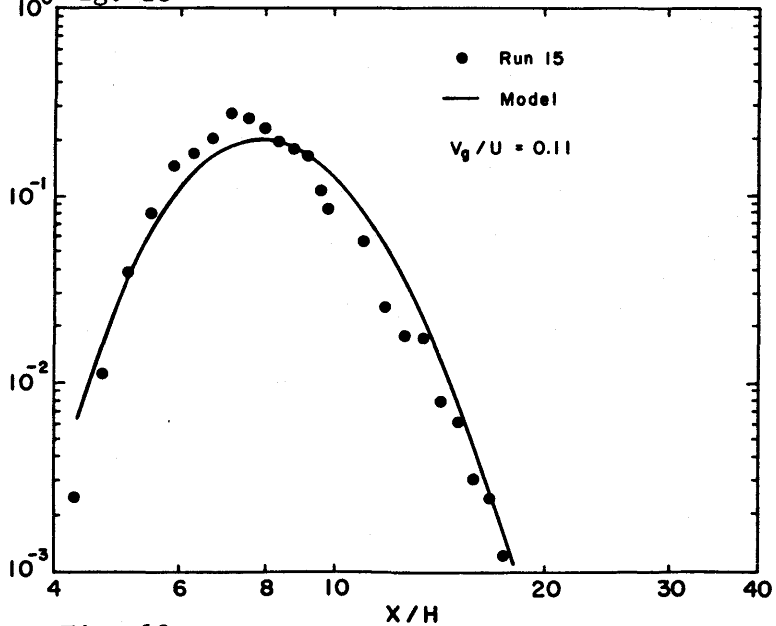

Fig. 20

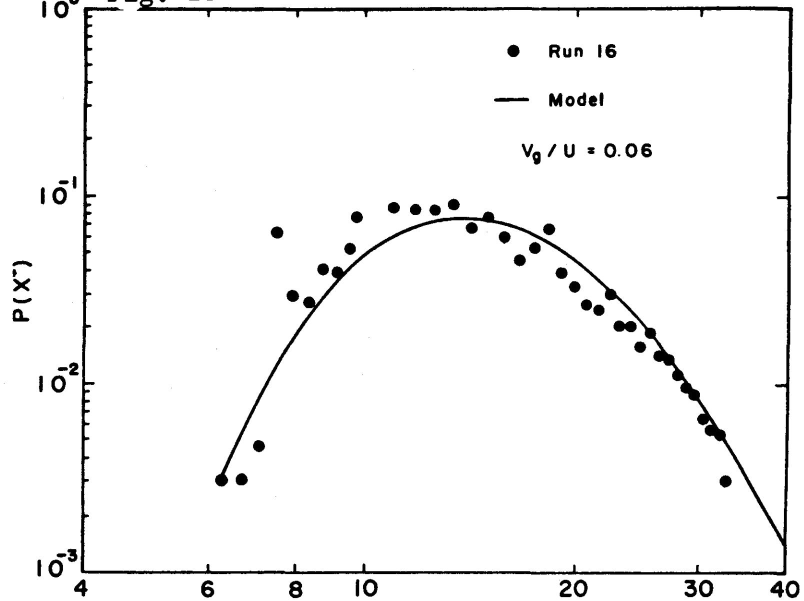

Fig. 19

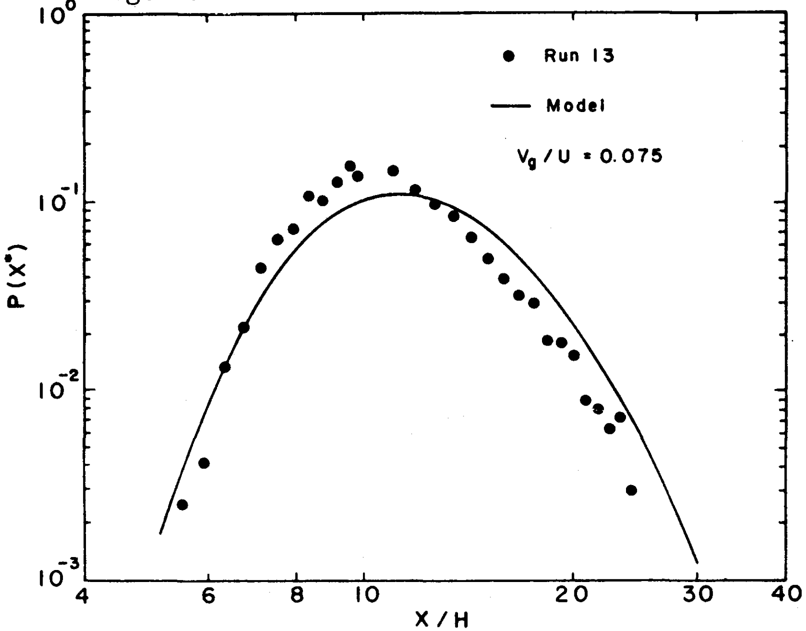

Fig. 21

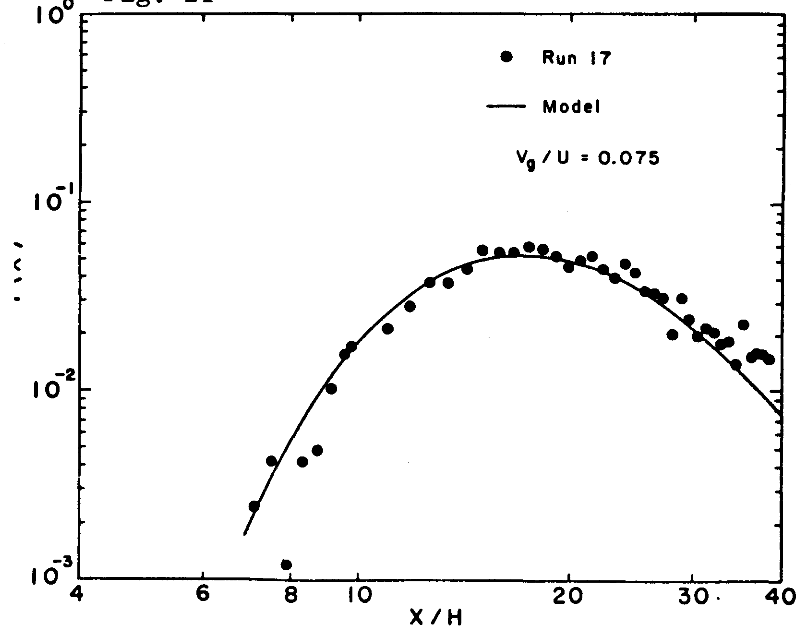

Figures 18-21. The longitudinal deposition of particles $P(x^*)$.

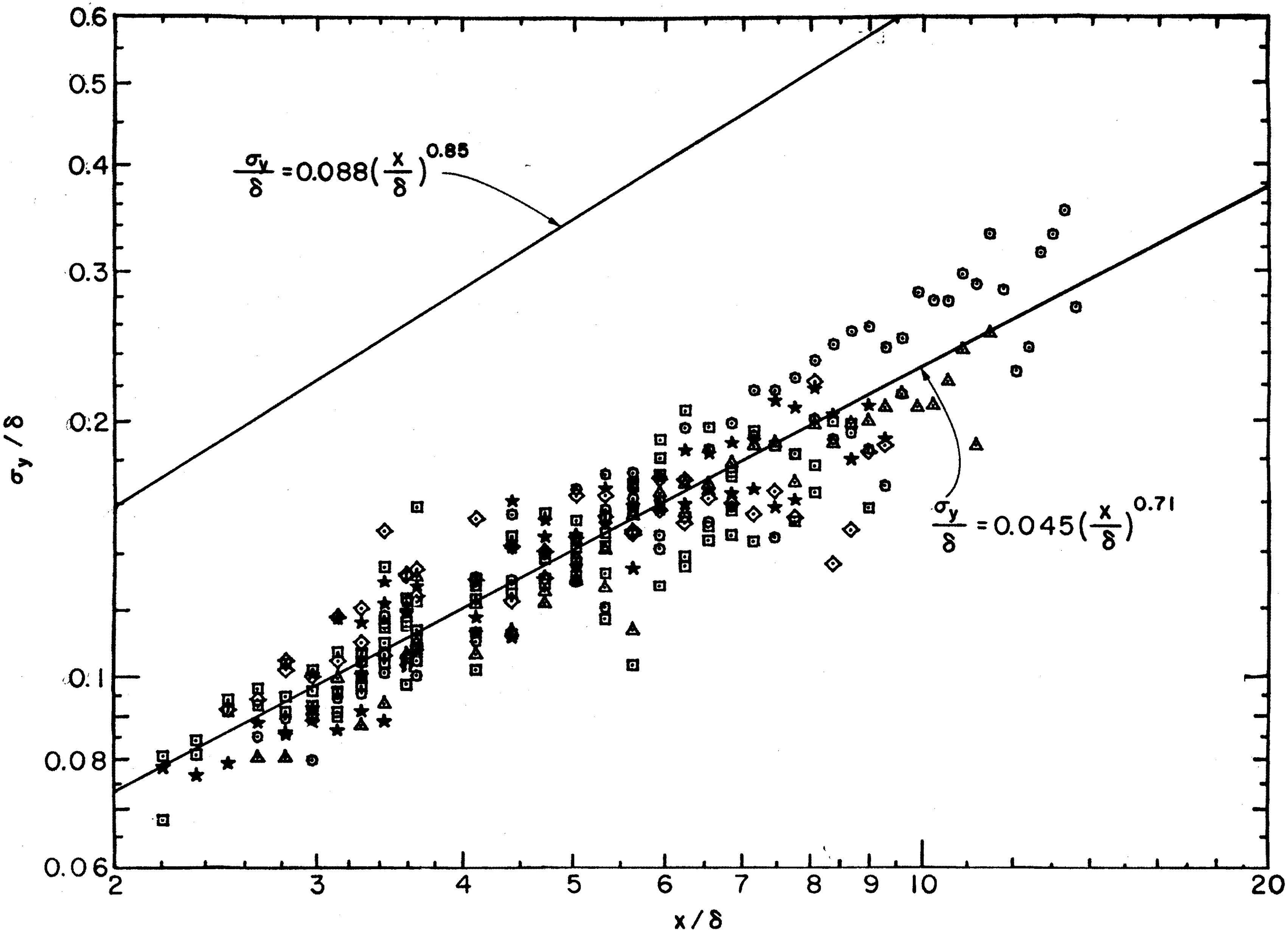

Figure 22. The lateral dispersion of particles (Runs 1-17).

of the maximum concentration in Run 5 was only slightly closer to the source.

The theoretical model appears to describe very well the general features of the longitudinal distribution of the particles. One notes, however, that the model predicts a maximum deposition at slightly larger distances than in the measurements.

If one uses, however, in the theoretical model a slightly higher velocity ratio, $V_g/U = 0.11$, for example, instead of 0.10, the agreement between the model and the data is highly improved, as shown in the figure.

One can attribute the differences between the measurements and the model to several causes:

(1) The approximate nature of the model. We have a priority estimated that the model will overpredict the distances at which the particles would deposit and pointed out that the model is not exactly mass consistent.

(2) An incorrect estimate of σ_z.

(3) Errors in the determination of U, V_g and h.

(4) A combination of the above factors.

Figure 13 shows the deposition distributions measured in Runs 6 and 7. The estimated mean relative fall velocity for these groups of particles was the same; $V_g/U = 0.1$. The value of V_g and therefore the Froude number V_g^2/gh was, however, larger than in the previous runs (Fr = 0.018 in Run 5, 0.024 in Runs 1, 2, and 3, 0.076 in Run 7 and 0.087 in Run 6). The two figures show a systematic change in the concentration profiles with the fall velocity or Froude number. In particular one observes a higher concentration value in Runs 6 and 7 at large values of x^*.

Some of the differences between the runs may be attributed to the factors mentioned earlier. It is quite possible that the average value of V_g/U in Runs 6 and 7 was closer to 0.9. There are, however, two additional factors which could have affected the diffusion of the particles having larger absolute values of V_g (Runs 6 and 7):

(1) The effect of the Froude number V_g^2/gh

(2) A possible effect of the larger nonuniformity of fall velocities in these groups (see section 4.2).

An increased Froude number is expected to decrease the fluctuations of the particles and thus to decrease σ_z. Such an effect should reduce the area on which the particles deposit and increase $P(x^*)_{max}$. Since we have observed in the experiments the opposite effect, we cannot attribute the change in the deposition pattern to the increased value of the Froude number. On the other hand, we have noted earlier that these groups had a much wider distribution of fall velocities, and as shown in Figure 11 a wider distribution could produce a similar effect to the one observed in Figure 13.

Figures 14-21 compare the measurements of the longitudinal distribution with prediction of the model for the rest of the runs. The Froude numbers for these runs were relatively small except for Run 14 (see Table 1). Indeed, one sees in Figure 17 that Run 14 produces slightly larger values of $P(X^*)$ at larger distances as observed earlier in Run 7.

Although the measurements at many locations deviate from those predicted by the model, the agreement between the experimental data and the model can be considered to be satisfactory, taking into consideration the limitations of the model.

5.3 The Measured Lateral Diffusion

Assuming that the lateral distribution of particles at a given distance x is approximately normal, we have calculated the value of $\sigma_y(x)$ at different values of x for the different runs. As noted earlier (see Figure 4), the number of particles at small and large distances from the source was not sufficient for obtaining a good estimate of σ_y from the standard deviation of the sample and we have thus omitted from the graph 70 data points (out of 385) at large and small distances from the source.

According to the assumption that $\sigma_y(x)$ for small particles is equal to σ_y for a passive tracer, and our further assumption that for a passive tracer in a neutrally stable flows $\sigma_y = f(\delta, x)$ and independent of h, as described in Eq. (39); or, $\sigma_y/\delta = e(x/\delta)^d$, we have plotted in Figure 22 the variation of σ/δ versus x/δ. (Note that δ was 1.0 m in all the experiments.) Although the experimental scatter in the figure is relatively large, it appears that the general trend of the data can be described by such a power law. However, as seen from the graph, the measured lateral diffusion of the particles is much smaller than the estimated value for passive tracers ($e = 0.088$ and $d = 0.85$, which were calculated using Briggs' data (1973).[1] Using a least-squares estimator, we have found that the particle data gives $e = 0.045$ and $d = 0.71$. When the 72 data points at large x/δ were included in the analysis, the values of d decreased slightly to 0.68 whereas the value of e did not change.

This very large difference between our estimate for passive tracers and the particles diffusion may be attributed to the following causes:

(1) The lateral dispersion in wind tunnels with finite widths, $b/\delta = 2$ in our case, can be much smaller than in atmospheric flows, as the wind tunnel simulates the mechanical turbulence and not the meandering of the mean velocity. This is particularly true for relatively smooth boundaries. Thus it is possible that our

estimate of σ_y for passive tracer is not applicable to this wind-tunnel simulation.

(2) As shown earlier, the response time of the falling particles to horizontal velocity fluctuations could be larger than their response to vertical velocity fluctuations. The Reynolds number of the falling particles was between 20 and 40. Thus, it is quite possible that although the vertical dispersion of the particle-plume is equal to that of a passive plume, the Froude number in the experiments was not sufficiently small to ensure the same equality between the lateral dispersion of passive tracers and the particles.

(3) Inspite of the relatively small fall velocity, the particles experienced a decreased diffusivity due to eddy crossing.

Lack of direct measurements of both σ_y and σ_z in the wind tunnel for passive plumes at the same flow configuration (roughness and Reynolds numbers), and lack of experiments at smaller Froude numbers, make it impossible to decide whether the good agreement between the longitudinal deposition in the theoretical model and in the experimental results is not partially due to the particular choice of σ_z and whether the failure of the model to describe the lateral diffusion is due to the generally reduced lateral diffusion in wind-tunnels or whether it is due to the decreases lateral diffusivity of the particles.

5.4 Conclusions and Recommendations

The deposition of particles with appreciable fall velocities emitted from elevated sources in a neutrally stable boundary layer was measured experimentally. The longitudinal distributions of the dimensionless cross-wind integrated concentration of the particles on the ground were described by a simple model, which assumes that the vertical spread of the particle plumes with small Froude numbers is equal to that of passive plumes except that the particles settle at a mean velocity V_g. The lateral spread rates of the particle plumes, however, were found to be smaller than those predicted of passive plumes.

It should be stressed, however, that the estimated values of σ_z and σ_y for passive plumes were estimated from field data and were not measured directly in the wind tunnel. Thus, it is recommended that similar experiments be carried out for a wider range of Froude numbers and relative fall velocities and that simultaneous measurements of σ_z and σ_y for passive tracers be carried at the same wind-tunnel configuration.

LITERATURE CITED

1. Briggs, G. A., (1973), In Handbook on Atmospheric Diffusion, by Hanna, S. R., Briggs, G. A., and Hosker, R. P., Jr. Technical Information Center, U.S. Dept. of Energy (1982).

2. Cermak, J. E., (1971), "Laboratory Simulation of the Atmospheric Boundary Layer," AIAA, Vol. 9, No. 9, pp. 1746-1749.

3. Cermak, J. E., (1975), "Application of Fluid Mechanics to Wind Engineering," ASME J. of Fluid Engineering, Vol. 97, Series 1, No. 1, pp. 9-38.

4. Cermak, J. E., (1981), "Wind Tunnel Design for Modelling of Atmospheric Boundary Layer," J. of Eng. Mech. Div., ASCE 107, No. EM3, 623-642.

5. Chamberlain, A. C., (1953), Aspects of Travel and Deposition of Aerosol and Vapor Clouds, Atomic Energy Research Establishment HP/R 1261, Harwell, Berkshire, England, 35 p.

6. Counihan, J., (1974), "Adiabatic Atmospheric Boundary Layers: A Review and Analysis of Data from the Period 1880-1972," Atmos. Env., Vol. 9, pp. 871-905.

7. Csanady, G. T., (1963), "Turbulent Diffusion of Heavy Particles in the Atmosphere," J. Atmos. Sci., Vol. 20, pp. 201. (Also see Pasquill (1973) section 3.7.)

8 Godson, W. L., (1958), "The Diffusion of Particulate Matter from an Elevated Source." Arch. Meteor. Geophys. Bioklim., Vol. 10, pp. 305-327.

9. Overcamp, T. J., (1976), "A General Gaussian Diffusion-Deposition Model for Elevated Point Sources." J. of Applied Meteorology, Vol. 15, pp. 1167-1171.

10. Pasquill, (1974), Atmospheric Diffusion, 2nd Edition, Halsted Press, New York.

11. Poreh, M. and J. E. Cermak, (1984), "Criteria for Wind-Tunnel Simulation of Particle Plumes in the Atmospheric Surface Layer," Proceedings of the 1984 CRDC Conference on Obscuration and Aerosol Research, Aberdeen Proving Ground, MD, 25-29 June, CEP-84-85MPJEC5.

12. Smith, F. B. and J. S. Hay, (1961),"The Expansion of Clusters of Particles in the Atmosphere," Q. J. R. Meteorol. Soc., 87(371):82-101. (Also see Pasquill (1974), section 3.7.)

13. Soo, S. L., (1967), "Fluid Dynamics of Multiphase Systems," Blaisdelle Pub. Co., Waltham, Mass.